2 (2026) 100106

Contents lists available at ScienceDirect

NAM Journal

journal homepage: www.sciencedirect.com/journal/nam-journal

Full Length Article

Advancing next-generation risk assessment for cosmetic ingredients: transferring the 10-step read-across framework from human to environmental safety using triclosan as a case study

Harald Streicher [a,*], Sanghamitra Mishra [b], Zakaria Naddi [a], Rita Fernandes [a], Monica Autiero [b], Sophia Krause [a], Avneet Kaur Suri [b], Celine De Roy [b], Andreas Schepky [a], Abdulkarim Najjar [a]

[a] Beiersdorf AG, Beiersdorfstrasse 1-9, 22529, Hamburg, Germany
[b] ToxMinds BV, Brussels, Belgium

ARTICLE INFO

Keywords:
Environmental risk assessment
Next-generation risk assessment
New approach methodologies
Triclosan
Read-across
In vitro to *in vivo* extrapolation
Cosmetics
Personal care products

ABSTRACT

Environmental risk assessment (ERA) has not yet undergone the shift toward new approach methodologies (NAMs), that has reshaped human health safety assessment. This study adapts the 10-step read across next generation risk assessment (NGRA) framework developed for cosmetic safety, to the environmental domain and applies it to triclosan (TCS), given its data richness and environmental relevance.

The framework consists of three tiers: Tier 0 for problem formulation and *in silico* screening; Tier 1 for bioavailability estimation and mode of action hypothesis formulation; and Tier 2 for refinement, hazard characterisation, risk quantification and uncertainty assessment. Four core principles are proposed for environmental NGRA: the assessments should (1) be exposure-anchored, (2) be mechanism-based, (3) have translatable thresholds, and (4) be both protective and transparent.

Exposure was assessed using a two-tier use-based predicted environmental concentration (PEC) approach. The lower tier applied a conservative aggregate cosmetic exposure scenario, yielding a screening PEC of 0.74 μg/L. This value exceeded both the ecological threshold of toxicological concern (ecoTTC) and Tier 0 read across thresholds, triggering refinement using year specific exposure data.

Integrated bioactivity, QIVIVE and conservation analysis identified lipid and steroid metabolism as the most sensitive pathways. Tier 2 yielded two NGRA predicted no effect concentrations (PNECs): a species sensitivity distribution (SSD)-based PNEC of 0.020 μg/L and a lowest environmental point of departure (ePoD)-based PNEC of 0.007 μg/L. Risk characterisation ratios (RCRs) were below 1 from 2019 onwards under both routes, supporting an environmental NGRA approach at least as protective as conventional ERA.

While the proposed framework has been demonstrated for an insecticide, this study extends it to a cosmetic ingredient, broadening the transferability of the 10-step framework for NAM-based ERA.

Introduction

Global production of chemicals has roughly doubled over the past two decades and is projected to double again by 2030, placing increasing demands on regulatory frameworks designed to ensure environmental safety (Alpizar et al., 2019). Environmental risk assessment (ERA) for aquatic ecotoxicology has traditionally relied on whole organism ecotoxicity studies, using one representative species from each of the three trophic levels: typically, a fish species, an aquatic invertebrate and a green alga. The effect thresholds derived from these studies, with the predicted no-effect concentration (PNEC) being the most widely used, form the basis of regulatory ERA under frameworks such as European Union Regulation on Registration, Evaluation, Authorisation and Restriction of Chemicals (EU REACH) and the Biocidal Products Regulation (BPR). At the same time, the growing number of chemicals requiring assessment, combined with increasing ethical and regulatory pressure to reduce vertebrate animal testing, has raised scientific and regulatory interest in complementing conventional

* Corresponding author.
E-mail address: harald.streicher@beiersdorf.com (H. Streicher).

https://doi.org/10.1016/j.namjnl.2026.100106
Received 29 May 2026; Received in revised form 25 June 2026; Accepted 26 June 2026
Available online 26 June 2026

ecotoxicological data with mechanistic and computational information (Di Nicola et al., 2023; Langan et al., 2024; Mitchell et al., 2023). This pressure is particularly high for cosmetic ingredients. Regulation (EC) No 1223/2009 (EU, 2009) prohibits animal testing carried out to support cosmetic safety in the EU, yet these same ingredients remain subject to environmental (ENV) data requirements under REACH (EU REACH, 2006) and, if applicable, the BPR (EU, 2012). As a result, generating new vertebrate ecotoxicity data to address the remaining ENV data gaps is highly constrained in practice. This, together - with the 3Rs (Reduction, Refinement and Replacement) expectations, in the scientific community, makes a structured new approach methodologies (NAMs)-based approach to ERA both practically necessary and scientifically timely (Di Nicola et al., 2023; Langan et al., 2024; Rivetti and Campos, 2023).

NAMs (including *in silico* models and *in vitro* assays), adverse outcome pathways (AOPs) and integrated approaches to testing and assessment (IATA) offer tools that can complement conventional ecotoxicological data in ERA. One area where NAMs bring specific value is in the assessment of cross-species biological relevance. Sequence conservation tools such as Sequence Alignment to Predict Across Species Susceptibility (SeqAPASS) can assess whether a molecular target identified in a cell-based assay is likely to be present and functional across a wide range of species, providing a mechanistic basis for extrapolation that goes beyond the standard three test organisms (LaLone et al., 2016). Mechanistic data from *in vitro* bioactivity platforms, mapped through AOP networks and enriched pathway analyses, can similarly help link molecular initiating events to established apical ecotoxicological endpoints across diverse taxa. Despite this potential, NAMs in ERA still lack a structured, tiered integration into regulatory assessment frameworks, in contrast to the progress made for human health (HH) over the past decade (Di Nicola et al., 2023; Langan et al., 2024; Rivetti et al., 2025).

The HH domain provides a working model worth building on. Next-generation risk assessment (NGRA) was outlined under the International Cooperation on Cosmetics Regulation (ICCR) as an exposure-led, hypothesis-driven approach that integrates *in silico, in chemico* and *in vitro* data to support safety decisions without new animal data. Nine core principles underpin this approach as described by Dent and colleagues: the overall goal is a human safety assessment; the assessment is exposure-led; the assessment is hypothesis-driven; the assessment is designed to prevent harm; the assessment follows an appropriate appraisal of all existing information; the assessment uses a tiered and iterative approach; the assessment uses robust and relevant methods and strategies; sources of uncertainty should be characterised and documented; and the logic of the approach should be transparently and explicitly documented (Dent et al., 2018). Alexander-White and colleagues translated these principles into a practical 10-step read-across (RAX) framework, which organises the assessment into Tier 0 (problem formulation and screening, Steps 1 to 4), Tier 1 (bioavailability and mode of action (MoA) hypothesis generation, Steps 5 to 6), and Tier 2 (targeted refinement, point of departure derivation using read across, and risk characterisation, Steps 7 to 10) (Alexander-White et al., 2022).

The practical value of this framework has been demonstrated through several published case studies, including caffeine (Bury et al., 2021), propylparaben (Ouedraogo et al., 2022), phenoxyethanol (Hewitt et al., 2022), benzyl salicylate (Ebmeyer et al., 2024), and daidzein (Najjar et al., 2024), which consistently reached the conclusion that the NGRA approach is at least as protective as the conventional approach using animal testing.

For environmental safety assessment, recent work has progressed beyond proof of concept and has already started to establish conceptual frameworks for integrating NAMs and mechanistic data into ERA decision making (Rivetti et al., 2025). With this study, we take a step further and present a structured end-to-end demonstration of the 10-step NGRA read across framework specifically adapted to the environmental domain for a cosmetic ingredient with a direct post-use wastewater-mediated aquatic exposure route. Triclosan is used as a case study.

Triclosan (TCS; 5-chloro-2-(2,4-dichlorophenoxy)phenol; CAS 3380–34–5) is a broad-spectrum antimicrobial agent used as a preservative in cosmetics, personal care products and household items; it is listed in Annex V, entry 25 of Regulation (EC) No 1223/2009. After consumer use, TCS has been repeatedly detected in surface waters, including at concentrations of potential ecotoxicological relevance, in part because wastewater treatment removal is incomplete (Bedoux et al., 2012; Halden and Paull, 2005). Measured surface water concentrations can reach the low-microgram per litre range near discharge points (Capdevielle et al., 2008). The compound has a self-classification of Aquatic Acute 1 (M factor: 100) and Aquatic Chronic 1, and both persistent, bioaccumulative and toxic (PBT) and endocrine disruption (ED) concerns are under active regulatory consideration through the ECHA Public Activities Coordination Tool (PACT) process (ECHA PACT, 2025). A known metabolite, methyl-triclosan, adds further complexity to the hazard profile because of its higher lipophilicity, higher bioaccumulation potential and greater environmental persistence relative to the parent compound (Bedoux et al., 2012).

This combination of cosmetic relevance, post-consumer aquatic exposure, data richness and MoA complexity made TCS a suitable compound for an exemplary case study of the environment NGRA (ENV NGRA) framework. Extensive ecotoxicological studies across the three standard aquatic trophic levels, covering chronic endpoints for fish, invertebrates and algae, are available in regulatory dossiers and public databases (ECHA CHEM, 2026; NICNAS, 2009; Oekotoxzentrum, 2021), together with mechanistic data high-throughput screening (HTS) platforms, including Toxicity Forecaster (ToxCast), high-throughput transcriptomics (HTTr), high-throughput phenotypic profiling (HTPP), and PubChem (Harrill et al., 2021; Nyffeler et al., 2020; Richard et al., 2021; US EPA, 2026c; Zdrazil, 2025). To test the framework, simulating a data poor substance, *in vivo* vertebrate data were deliberately excluded from the Tier 2 environmental point of departure (ePoD) derivation. This would allow to specifically assess whether NAMs, integrated with read-across and the available invertebrate and algal data, are sufficient to reach a protective risk conclusion.

The study had four specific objectives: (1) to develop an ENV NGRA decision framework derived from the HH 10-step NGRA approach; (2) to demonstrate the framework using TCS as a case study integrating tiered exposure and bioactivity data; (3) to compare the protectiveness of the NGRA-derived conclusions with those derived from traditional ERA; and (4) to characterise the main sources of uncertainty and consider their implications for regulatory implementation.

Materials and methods

Comparison of the human health 10-step framework with the environmental NGRA

Each step of the HH 10-step NGRA framework (Alexander-White et al., 2022; Najjar et al., 2024) was reviewed for direct applicability, required adaptation, or need for domain-specific replacement when transferred to the environmental domain. The mapping is summarised in Table 1. The core three-tier architecture was applied without structural changes: Tier 0 for problem formulation and data collation, Tier 1 for bioavailability and MoA hypothesis building, and Tier 2 for targeted testing, ePoD derivation and risk characterisation. Some elements of the HH workflow could be transferred directly at the level of assessment approach, but several steps required domain-specific modification of both data inputs and decision criteria. The main adaptations concern Steps 1, 5 and 6. In the HH framework, Step 1 defines the use and exposure scenario in terms of human use patterns and systemic exposure, whereas in the environmental context this step is adapted to estimate environmental release and derive predicted environmental concentrations (PECs) on the basis of product use, emission to wastewater, and environmental fate assumptions. In the HH framework, Step 5 relies on human physiologically based kinetic (PBK) modelling with

Table 1
Mapping of the 10-step human health NGRA read-across framework (Alexander-White et al., 2022; Najjar et al., 2024) to the environmental NGRA framework developed in this study, indicating the nature of adaptation required for each step.

Steps	HH NGRA	ENV NGRA	Adaptation
Step 1	• Define use and exposure scenario • Estimate human systemic dose	• Define use and exposure scenario • Derive lower tier PEC using monitoring data or fate modelling	• Human systemic dose replaced by aquatic PEC derived from use-based emission modelling
Step 2	• Characterise the molecular structure • Classify using the threshold of toxicological concern (TTC) approach	• Characterise the molecular structure • Profile the MoA using *in silico* MoA profiling • Classify using the ecoTTC approach	• Human TTC thresholds replaced by ecoTTC values calibrated to aquatic species sensitivity
Step 3	• Collate existing human toxicity data • Identify data gaps	• Collate ecotoxicity, ED and regulatory threshold data • Identify data gaps	• Endpoint scope extended from human toxicity to aquatic ecotoxicity
Step 4	• Identify structural analogues for RAX • Assess physicochemical and toxicological similarity	• Identify structural analogues for RAX • Assess ecotoxicological similarity	• Similarity criteria extended to include ecotoxicological endpoints and aquatic fate properties
Step 5	• Estimate human systemic bioavailability using PBK modelling with dermally relevant toxicokinetic parameters	• Estimate aquatic bioavailability • Apply QIVIVE factor derived from bioconcentration factor (BCF) and intrinsic clearance using one-compartment PBK model	• Human PBK modelling replaced by aquatic QIVIVE • Biokinetic correction to account for uptake from water rather than dermal absorption
Step 6	• Generate MoA hypothesis using HTS data, ToxCast	• Generate MoA hypothesis using HTS data, aquatic bioactivity databases, AOP networks, SeqAPASS for cross-species susceptibility, and KEGG/Reactome pathway analysis	• Human pharmacological and bioactivity assays replaced by ecotoxicological MoA frameworks and cross-species computational tools • Mammalian data retained if evolutionary conservation is supported
Step 7	• Targeted *in vitro* testing to strengthen MoA hypothesis or to refine biokinetics, if needed	• Targeted NAMs and biokinetic refinement if needed • No new whole-organism vertebrate testing generated	• Gap analysis for targeted ecotoxicological NAMs and human/mammalian NAMs if conservation is demonstrated, with QIVIVE integration for bioactivity-to-exposure conversion
Step 8	• Read-across to derive the human PoD using benchmark dose modelling or no-observable adverse effect level (NOAEL)	• Derive environmental PoD (ePoD) using species sensitivity distribution (SSD) or the lowest-PoD approach (with data either from the substance itself or data from read across substances)	• Human PoD derivation replaced by ePoD with additional approach of using SSD
Step 9	• Calculate margin of safety (MoS) or bioactivity exposure ratio (BER) • Compare internal exposure against PoD	• Refine PEC value using product category and year specific market data • Calculate NAM-derived PNECs (either PNEC NAMs-SSD or PNEC NAMs-lowest) • Compare external exposure with PEC to derive risk characterisation ratio (RCR)	• Internal exposure metric (BER/MoS) replaced by RCR • Effect threshold compared against environmental water concentration rather than internal systemic exposure
Step 10	• Assess confidence and document uncertainties • Benchmark NAM-derived conclusions against traditional ERA outputs	• Assess confidence and document uncertainties • Benchmark NAM-derived conclusions against traditional ERA outputs	• Same approach for both HH and ENV

dermally relevant bioavailability parameters; in the environmental context, this becomes quantitative *in vitro* to *in vivo* extrapolation (QIVIVE), using aquatic organism PBK models and bioconcentration factors. Step 6, which supports MoA hypothesis, follows the same reasoning but it is informed by ecotoxicological AOP networks (Ankley et al., 2010), SeqAPASS for cross-species susceptibility assessment (LaLone et al., 2018, 2016) and Kyoto Encyclopedia of Genes and Genomes (KEGG), Reactome (Kanehisa and Goto, 2000) and Gene Ontology (GO) (Aleksander et al., 2023) pathway analysis applied to relevant aquatic taxa rather than human tissues (Ankley et al., 2010; LaLone et al., 2018, 2016).

Table 1 and Fig. 1 serve complementary rather than duplicate purposes. Table 1 provides the conceptual mapping between the established human health NGRA read-across framework and its environmental adaptation, identifying which elements were transferred directly and which required domain-specific modification. Fig. 1, in contrast, presents the operational ENV NGRA workflow used in the case study, including tier progression, decision points and exit criteria. The table therefore explains what was adapted from the human health framework, whereas the figure explains how the adapted environmental framework is applied in practice.

Overview of the environment NGRA framework

The ENV NGRA framework moves through three tiers of quantitative risk characterisation assessment, each with defined exit criteria. The overall workflow is illustrated in Fig. 1.

Tier 0 includes problem formulation and existing data. The use scenario and exposure conditions are defined, and available ecotoxicity data are collected. The lower tier PEC is compared against the applicable ecoTTC and any analogue-derived PNEC. If PEC is below either threshold, the assessment exits with a low-concern conclusion.

Tier 1 focuses on the MoA hypothesis on the basis of NAMs results. Bioavailability modelling and *in vitro* bioactivity data are analysed to develop a mechanistic MoA hypothesis, from which a preliminary NGRA-based PNEC is derived. If the PEC is lower than this PNEC(NGRA) value, the assessment may exit at this stage.

Tier 2 is related to targeted refinement and risk characterisation. Additional NAM and biokinetic data are generated as needed; the ePoD is refined; a final PNEC—NGRA is derived via SSD or the lowest-no observable adverse effect concentration (NOAEC) approach; the risk characterisation ratio (RCR = refined PEC/PNEC—NGRA) is calculated; and uncertainties are identified, characterised and documented.

The context-of-use of the ENV NGRA framework is a prospective, decision-oriented environmental safety assessment for cosmetic and other down-the-drain ingredients where new vertebrate testing is not generated and where existing ecotoxicity data, NAM-derived bioactivity information, exposure modelling and uncertainty analysis need to be integrated into a transparent risk conclusion. The framework is not proposed as a stand-alone replacement for all regulatory ERA contexts,

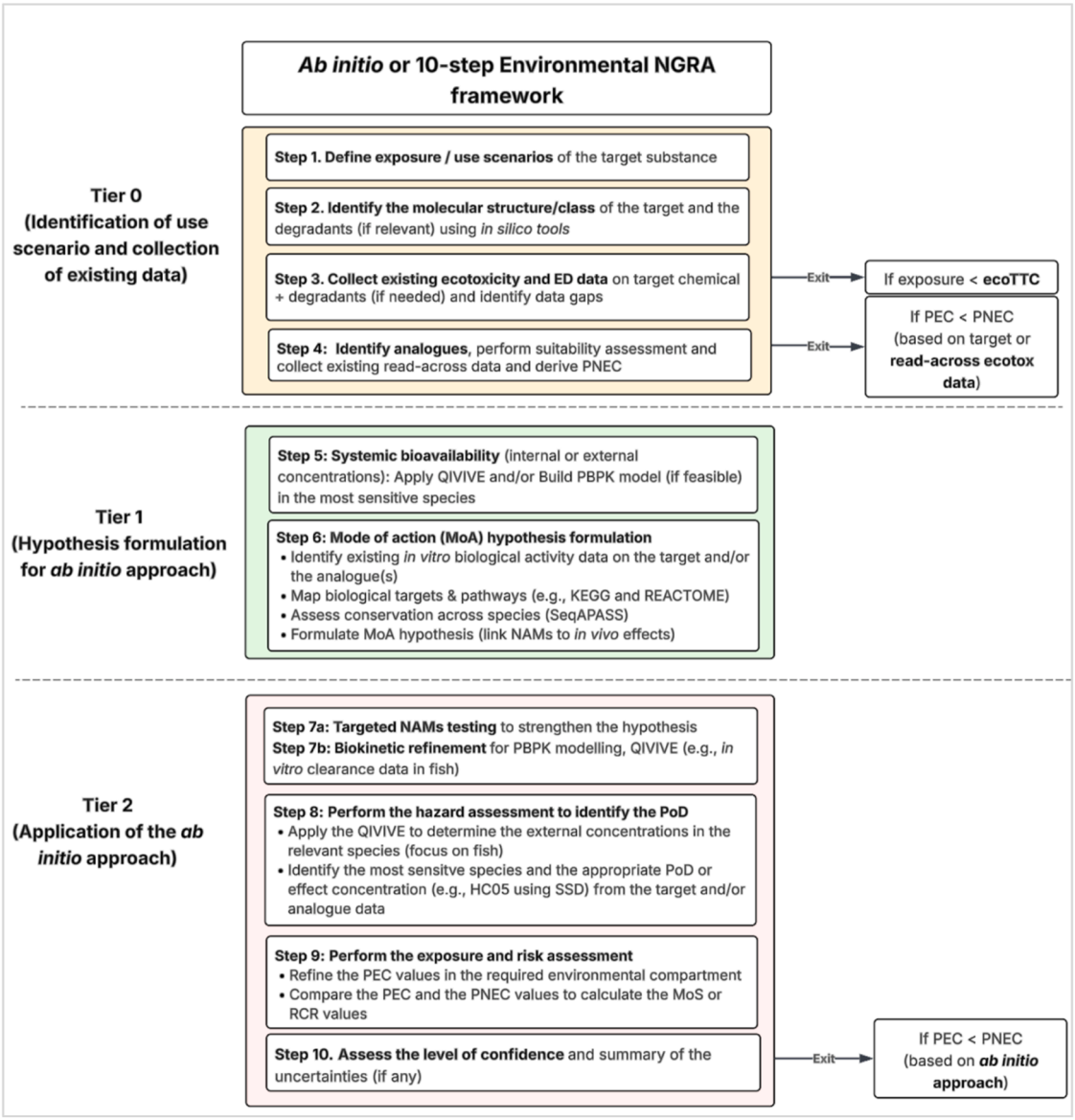

Fig. 1. Environmental Next Generation Risk Assessment (Env NGRA) workflow.
The figure presents the operational application of the adapted 10-step framework, including tier progression, decision points and exit criteria. Conceptual mapping of the human health NGRA framework to the environmental context is provided separately in Table 1.

but as a structured approach for deriving exposure-anchored and mechanistically informed environmental safety decisions.

Minimum evidence requirements depend on the tier at which the assessment exits. Tier 0 requires chemical identity, use and release information, physicochemical properties, *in silico* profiling, an initial PEC, and either an ecoTTC or an analogue-based threshold. Tier 1 and Tier 2 additionally require a curated bioactivity dataset (targeted molecular assays, broad-coverage data such as transcriptomics and cellular phenotype data), a biokinetic translation step (*e.g.*, QIVIVE) where *in vitro* data are used quantitatively, an assessment of cross-species relevance for molecular targets used as hazard anchors, and explicit documentation of uncertainty and confidence.

Tier 0: Identification of use scenario and collection of existing data (Steps 1–4)

Step 1: exposure / use scenarios of the target substance

The exposure assessment was developed as a two-tier use-based framework, which combines the assessment approach of the Scientific Committee on Consumer Safety (SCCS) for consumer exposure with the emission characterisation commonly applied for human hygiene products (Product Type 1) in the BPR context. In Step 1, exposure was first represented by a conservative lower tier screening PEC for Tier 0 decision making. This lower tier was designed to test whether a low concern conclusion could be reached under protective aggregate exposure assumptions. If the Tier 0 exit criteria were not met, the exposure estimate was refined in Step 9 using product category specific and year specific market data for final risk characterisation.

For the lower tier screening assessment, TCS was assumed to occur across the aggregate cosmetic product basket, rather than being restricted to the specific product categories identified in market datasets. The SCCS aggregate cosmetic product use value of 17.4 g/person/day was used as the daily product amount. A TCS concentration of 0.3% was applied, corresponding to the maximum concentration used for the main cosmetic product categories considered in the regulatory assessment. A generic product occurrence factor of 5.2% was considered, based on the highest occurrence reported for a relevant daily use cosmetic category in the Danish EPA shop survey (Danish EPA, 2016),

namely deodorants. The fraction of inhabitants using the aggregate product basket was set at 100%. This lower tier assumption was selected to provide a conservative screening PEC while avoiding the unrealistic assumption that all cosmetic products contain TCS.

The lower tier local emission to wastewater was calculated as follows:

$$Elocal = Q_{aggregate} \times C \times F_{occ} \times F_{inh} \times F_{STP}$$

Where:
$Q_{aggregate}$ = Aggregate cosmetic product use value
C = concentration of TCS
F_{occ} = generic fraction of products containing TCS
F_{inh} = fraction of inhabitants using product category i
F_{STP} = fraction released to sewer after use.

The numerical input parameters used for the lower tier calculation were $Q_{aggregate}$= 17.4 g/person/day, C = 0.3%, F_{occ}= 0.052, F_{inh}= 1 and F_{STP}=1. For Tier 0, the distribution of TCS during wastewater treatment was not parameterised from monitoring data, but it was derived using the EUSES SimpleTreat module. The SimpleTreat-derived STP distribution was then applied within EUSES together with the local environmental dilution assumptions to calculate $PEC_{surface\ water}$. The refined exposure calculation using product category specific occurrence, user prevalence and year specific market data is described in Step 9.

Step 2: identification of the molecular structure/class of TCS and the corresponding degradants

The molecular structure and chemical class of TCS and its principal degradants were characterised, using *in silico* profiling tools. The characterisation covered the parent compound, its known degradant methyltriclosan, and the biodegradation products predicted by the Swiss Federal Institute of Aquatic Science and Technology – Biocatalysis/Biodegradation Database (EAWAG-BBD) pathway tool (EAWAG, 2026). The transformation products were included in the profiling because environmental degradation can generate metabolites with different persistence, bioaccumulation, or toxicity profiles compared to the parent compound. Therefore, *in silico* PBT screening was performed to determine whether any transformation product warranted separate consideration as a driver of aquatic hazard.

MoA profiling was carried out using two *in silico* platforms. The first is the EnviroTox Consensus MoA tool, which integrates predictions from the Ecological Structure–Activity Relationships model (ECOSAR), the Toxicity Estimation Software Tool (TEST), the Assessment Tools for the Evaluation of Risk database (ASTER), the Optimized Approach based on Structural Indices Set model (OASIS), and the Verhaar scheme (Verhaar), to generate a consensus MoA classification (EnviroTox, 2026). The second is the OECD QSAR Toolbox v.4.7 (MechoA 1.2), using the 'iSafeRat MoA', the 'OASIS acute aquatic toxicity MoA', the 'Verhaar (Modified) and the 'ECOSAR acute aquatic toxicity classification' profilers (OECD, 2024). Results from both platforms were used to establish a consensus MoA classification. The ecoTTC was then selected on the basis of the MoA classification, using the tabulated thresholds of De Wolf and colleagues for non-reactive and narcotic compounds (de Wolf et al., 2005), and Gutsell and colleagues for surfactants (Gutsell et al., 2015). If an estrogenic mode of action was identified as the primary endocrine mechanism, estrogenic ecoTTC threshold (Gross et al., 2010) was applied in place of the standard narcosis-based thresholds. The lower tier PEC derived in Step 1 was compared against the applicable ecoTTC to determine whether a low-concern conclusion could be reached at this step, or whether the assessment needed to proceed to further tiers.

Step 3: ecotoxicity data collection and identification of data gaps

Available ecotoxicity and endocrine disruption data for TCS were compiled from the ECHA REACH registration dossier (ECHA CHEM, 2026), national regulatory assessments from the National Industrial Chemicals Notification and Assessment Scheme (NICNAS, Australia), the Institut National de l'Environnement Industriel et des Risques (INERIS, France), the Danish Environmental Protection Agency (Danish EPA), and the Scientific Committee on Health, Environmental and Emerging Risks (SCHEER), as well as the Oekotoxzentrum Environmental Quality Standard (EQS) dossier.

A systematic data gap analysis was conducted to identify whether the existing regulatory dataset provided a sufficient basis for a low-concern conclusion at Tier 0. For the purposes of this case study, existing *in vivo* vertebrate ecotoxicity data for TCS were deliberately excluded from the Tier 0 to Tier 2 assessment to simulate the regulatory situation faced by cosmetic ingredient assessors, who cannot generate new vertebrate ecotoxicity data under Regulation (EC) No 1223/2009. This allowed the case study to specifically test whether a NAMs-based approach combined with invertebrate and algal data is sufficient to reach a protective risk conclusion.

Step 4: identification and evaluation of potential analogues, collection of read-across data and PNEC derivation

Structural analogues of TCS were identified through similarity searches using the OECD QSAR Toolbox, together with a targeted literature review. Candidate analogues were evaluated against four criteria: 1) structural similarity and common functional groups, 2) the presence of common structural alerts related to the MoA; 3) common physicochemical properties; and 4) the likelihood of common breakdown products through biotransformation or abiotic degradation processes. Potential analogues fulfilling these criteria were further assessed for the availability of relevant ecotoxicity data. The most suitable analogue was selected on this basis, and its data were used to derive a provisional PNEC for TCS, with appropriate assessment factors applied according to data availability and dataset quality. As mentioned above, existing *in vivo* vertebrate ecotoxicity data for TCS were deliberately excluded from the Tier 0 analogue-based PNEC derivation, with the selected analogue serving as the primary source for the vertebrate data component. All other ecotoxicity data, covering invertebrate and algal endpoints, were taken directly from TCS.

Tier 1: Hypothesis formulation for *ab initio* approach (Steps 5–6)

Step 5: bioavailability estimation and QIVIVE factor derivation

In vitro effect concentrations from cell-based assays are nominal concentrations applied to culture medium and are not directly comparable to external aqueous concentrations in the environment. Quantitative *in vitro-in vivo* extrapolation is therefore required before the comparison of *in vitro* bioactivity data with conventional ecotoxicological endpoints or with PEC values derived in Step 1. As presented in the conceptual model by Mackay and colleagues (Mackay et al., 2014), external exposure concentrations can be linked to internal dose via bioconcentration. The BCF represents the ratio of the steady-state concentrations in the living organism and that in the surrounding water (*i.e.*, $C_{organism}/C_{water}$), meaning that the BCF value can provide a conversion factor between external water concentration and internal organism concentration. The QIVIVE factor can be estimated using the equation: QIVIVE factor ≈ 1 / BCF.

For BCF calculation, we used a one-compartment modeling approach (Krause and Goss, 2020) implementing experimentally determined hepatic clearance data: intrinsic hepatic clearance (Clint) for TCS was measured as 39.1 μL/min/10^6 hepatocytes at 1 μM, using rainbow trout hepatocytes (RT-HEP) (Black et al., 2021). The intrinsic hepatic clearance value and an assumed log Kow of 4.9 were used as input parameters for the one-compartment model for BCF prediction (Krause and Goss, 2020) for a fish with bodyweight of 10 g and 5% body lipid.

This approach is consistent with an established practice in HH NGRA (Wetmore et al., 2012; Yoon and Clewell, 2016). The derived factor was

subsequently applied to the *in vitro* bioactivity data collated in Step 6 to convert nominal effect concentrations to external aqueous concentration equivalents (μg/L), placing both data streams on a common concentration basis for direct comparison.

Step 6: MoA hypothesis formulation

The generation of Tier 1 hypothesis required the assembly and systematic curation of a bioactivity dataset for TCS, followed by pathway and target mapping to formulate a mechanistic hypothesis, which links the molecular-level activity to apical ecotoxicological endpoints.

Data collection: Bioactivity and ecotoxicity data for TCS were retrieved from high-throughput screening platforms, omics datasets, curated ecotoxicity databases, toxicogenomic resources and targeted literature searches. These included ToxCast/Tox21, HTTr, HTPP, PubChem BioAssay, EnviroTOX (Connors et al., 2019), USEPA ECOTOX (Olker et al., 2022), ETOX (Briggs et al., 2015), NORMAN (Dulio et al., 2020), CTD (Davis et al., 2023) and peer-reviewed literature sources. The full list of data sources, data types, endpoint metrics and key references is provided in **Supplementary Data 2, Table S7**. The compiled *in vivo* aquatic toxicity endpoints from EnviroTOX, USEPA ECOTOX, ETOX and NORMAN are provided in **Supplementary Data 1**. In the main text, the subsequent sections focus on the curation, harmonisation and decision-relevant use of these data streams for MoA hypothesis formulation, pathway enrichment, ePoD derivation and risk characterisation.

Data curation: Data curation was conducted using a harmonised workflow across all data streams. In general, duplicate records, entries lacking an interpretable PoD, non-comparable activity descriptors (*e.g.*, IC_{90}, Ki, Kd and MIC_{90}), inactive or inconclusive assay outcomes, and records not relevant to the assessment context (*e.g.*, plant, bacterial and yeast studies) were excluded. In case multiple timepoints or concentrations were reported for a given endpoint, only the entry associated with the lowest effect concentration was retained to only include the most sensitive response. Additional source-specific curation steps were applied to high-throughput bioactivity, omics and ecotoxicological datasets to ensure consistency and comparability of effect descriptors across the different data streams. A detailed description of all source-specific curation steps is provided in the **Supplementary Data 2** (**Table S1**).

All remaining entries from these databases were consolidated into a single dataset and harmonised to ensure consistency: specifically, effect concentrations were converted into μg/L and μM; the endpoint descriptions were aligned using the same terminology, and the LOEC values were converted into NOEC values, using a factor of 2 for long-term ecotoxicological studies.

Given the data richness of TCS, a pragmatic approach was taken for the reliability evaluation. Reliability was assessed using the Klimisch scoring system (Klimisch et al., 1997), which classifies studies on a four-point scale from reliable without restriction (1) to not assignable (4). For each taxonomic group, up to three studies representing the lower end of the effect concentration range were selected for a detailed reliability assessment. Priority was given to the most sensitive endpoints, as these are most likely to influence the final ePoD and, consequently, the risk characterisation outcome. All the curation criteria and stepwise record counts are provided in the **Supplementary Data 2** (**Table S1**). The selected entries were classified by taxonomic group (algae, aquatic invertebrates, terrestrial invertebrates, aquatic vertebrates, lower vertebrates, birds and mammals), test type (ecotoxicological study, bioactivity, transcriptomics, proteomics and metabolomics), and effect group (including endpoints from mortality and growth to gene expression, physiology, cell stress and receptor activity). The seven taxonomic groups reflect the scope of the curated dataset, which extended beyond the three standard aquatic test organism groups to include terrestrial invertebrates, lower vertebrates (amphibians and reptiles), avians and mammals, as these provided additional mechanistic and pathway-level evidence relevant to the MoA characterisation. Lower vertebrates, specifically amphibians, were included given the direct aquatic exposure of larval life stages and their established sensitivity to endocrine-active substances, particularly through thyroid-mediated pathways (Kloas et al., 2009; Scholz et al., 2013). Within the terrestrial invertebrate group, data from *Caenorhabditis elegans* were included as a mechanistic line of evidence, given that its stress-response and metabolic pathways are broadly conserved across invertebrate and vertebrate taxa (Leung et al., 2008; Queiros et al., 2019), and its apical toxicity endpoints correspond reasonably well with those of standard aquatic test organisms (Crombie et al., 2026; Hunt, 2017). Although *C. elegans* is a soil-dwelling nematode, its ecotoxicological studies are routinely conducted in aqueous medium, supporting its inclusion in this context. Mammalian and human datasets were included on the basis that molecular targets identified in mammalian cell-based assays are frequently conserved across vertebrate taxa, including fish and amphibians (LaLone et al., 2016; Margiotta-Casaluci et al., 2024); where such conservation exists, mammalian bioactivity data can serve as a biologically plausible line of evidence for cross-species hazard characterisation (ECHA/EFSA, 2018; LaLone et al., 2018). Full details of the effect category classification scheme are provided in the **Supplementary Data 2** (**Table S2**). The resulting harmonised multi-source dataset is hereafter referred to as the integrated TCS hazard dataset and forms the basis for all subsequent steps of the NGRA assessment, including the derivation of PNEC—NGRA values in Step 8.

MoA hypothesis: The MoA of TCS was characterised based on the complete curated NAMs dataset, which included effect groups like enzyme activity, receptor activity, protein-level measurements, cell stress indicators, physiological endpoints and gene expression data across all taxonomic groups. Apical ecotoxicological endpoints were not included at this stage, since the MoA characterisation requires mechanistic information including the molecular and cellular events underlying the response, rather than organism-level outcomes. The findings were interpreted based on established toxicological knowledge from literature review to assess whether the molecular targets and biological pathways identified were consistent with the apical effects observed in the conventional ecotoxicity studies.

Biological target and pathway mapping was conducted using three complementary pathway and ontology databases – KEGG, Reactome and GO. KEGG provided organism-specific metabolic and signalling pathway maps, identifying which functional pathway(s) was over-represented within the TCS-responsive gene set (Kanehisa and Goto, 2000). Reactome provided a more granular, reaction-level view of biological processes - for example, it resolves individual regulatory events such as phosphorylation or sumoylation of nuclear receptors as discrete steps, whereas KEGG depicts these at a schematic pathway level without resolving each modification separately (Milacic et al., 2024). GO enrichment was used as confirmatory and supplementary evidence (Aleksander et al., 2023). Biological process terms indicated the broader functional context of the response; cellular component terms identified subcellular localisation; and molecular function terms specified the biochemical activities of the gene products concerned.

To provide mechanistic confirmation of the MoA hypothesis, gene-based pathway enrichment analysis (over-representation analysis) was performed separately for each organism (*i.e., Homo sapiens, Danio rerio,* and *C. elegans*) using the clusterProfiler package (v.4.10.1) (Yu and He, 2016) and ReactomePA (v.1.46.0) in R (v.4.3.3) (Yu and He, 2016), with Benjamini–Hochberg correction, which was applied to control the false discovery rate (adjusted p-value < 0.05). The enriched terms from each database and organism were then compared across species to identify pathway categories that were consistently represented and those that were species- or test-system-specific. Individual enriched terms were grouped into higher-level macro-pathway categories by expert interpretation of the hierarchical clustering output (treeplots) and by consolidating terms describing the same biological process that

appeared under different nomenclature across KEGG, Reactome and GO. For each pathway category, the lowest effect concentration per taxonomic group was identified from the curated dataset, with *in vitro*-derived values QIVIVE-corrected as described in Step 5. The enriched pathways were interpreted based on established toxicological knowledge from literature review and expert judgement to assess whether the biological targets and pathways identified in the bioactivity dataset were consistent with the apical effects observed in conventional ecotoxicity studies.

The overall most sensitive biological target was selected as the candidate to determine cross-species conservation and for the ePoD derivation in Step 8. Cross-species conservation of this target was assessed using SeqAPASS (LaLone et al., 2018, 2016), with the overall objective to evaluate whether the identified molecular target was structurally and functionally conserved across the key ecotoxicological test organisms, thereby supporting the biological plausibility of a similar effect across species.

The MoA hypothesis was formulated by integrating these lines of evidence: full-dataset bioactivity characterisation, gene-based pathway enrichment analysis as confirmatory evidence lowest-effect concentration analysis per taxonomic group, and cross-species sequence conservation.

Tier 2: Application of *ab initio* approach (Steps 7–10)

Steps 7a and 7b: targeted testing and biokinetic refinement

The existing integrated TCS hazard dataset was analysed to determine whether additional targeted NAM data were needed to confirm the MoA hypothesis. If gaps were identified, targeted ecotoxicological NAMs testing and human/mammalian NAMs (if conservation is demonstrated) was considered — including thyroid function, estrogen receptor (ER) activity and metabolic disruption assays — was considered in the context of the identified MoA. QIVIVE was applied using the parameters established in Step 5 to convert *in vitro* bioactivity concentrations to aquatic exposure-equivalent values before the integration with the *in vivo* ecotoxicity data. No additional vertebrate data were generated or considered at this stage; consistent with the case study design.

Step 8: hazard assessment and identification of ePoD

The ePoD was derived from the integrated TCS hazard dataset by two different approaches: a lowest-effect-concentration approach yielding PNEC—NGRA-lowest and a species-distribution-based approach yielding PNEC—NGRA-SSD.

For the lowest-PoD approach, effect concentrations from the integrated dataset were compared across taxonomic groups after QIVIVE correction when applicable, and the lowest value identified as the conservative ePoD. PNEC—NGRA-lowest was derived by applying an assessment factor to this value.

The SSD was developed across the full taxonomic range of the integrated dataset, combining *in vivo* aquatic ecotoxicity values, read-across-derived vertebrate values, and QIVIVE-corrected NAM-derived effect concentrations (**Step 5**). Effect descriptors (NOAEC, EC_{10}, AC_{50} and LEC) corresponded to different positions on the concentration-response curve and were treated as conservative screening-level thresholds without further normalisation, consistent with the approach previously described (Paul Friedman et al., 2020). The SSD was fitted using the US EPA SSD Toolbox v.1.1 (Etterson, 2020) with six distributions (Weibull, Burr, log-normal, log-logistic, log-triangular and log-Gumbel) estimated by maximum likelihood, and the best-fitting model selected by the corrected Akaike Information Criterion (AICc). PNEC—NGRA-SSD was derived by applying an assessment factor to the resulting hazardous concentration for 5% of species (HC_{05}), *i.e.*, the concentration at or below which 95% of species are protected, to account for residual uncertainty.

Dose descriptor heterogeneity is addressed as a source of uncertainty in Step 10.

Step 9: exposure and risk assessment

For the final risk characterisation, the lower tier screening PEC was refined in Step 9 by replacing the conservative aggregate exposure assumptions with product category specific use values, year specific TCS occurrence data and category specific user prevalence. Only product categories compatible with the regulatory use pattern of TCS and supported by market occurrence data were included. TCS was, therefore, not treated as a generally permitted preservative across all cosmetics, but as a preservative restricted to specific cosmetic product categories under Annex V, entry 25 of Regulation (EC) No 1223/2009 (EU, 2009). For the present case study, Mintel indicated occurrence in colour cosmetics, skin care, soap and bath products, and deodorants in Europe. A TCS concentration of 0.3% was used as a conservative upper bound for the product categories modelled here. Product specific daily use amounts were based on SCCS default exposure values. For colour cosmetics, the daily use input was defined as the arithmetic mean of the SCCS values for liquid foundation, make up remover, lipstick, eye makeup, mascara, and eyeliner. For skin care, the daily use input was based on face cream and hand cream only. Body lotion was excluded from the refined calculation (see **Supplementary Data 3**), because TCS should not be treated as an acceptable body lotion scenario in light of the SCCS opinions, which identified body lotion as a major contributor to aggregate exposure and did not support its safe use in that product type (EU, 2024; SCCS, 2011, 2022).

In the refined exposure assessment, occurrence and prevalence were incorporated explicitly. Category specific TCS occurrence was derived from Mintel, and the fraction of inhabitants using each category was represented by the highest country specific user prevalence identified in the Mintel surveys, in order to retain a conservative European consumer use scenario (Mintel, 2026). Since the Mintel data are proprietary, the underlying percentages are not reproduced here; however, the same calculation structure was applied consistently across categories. The calculation was performed separately for each year for which annual Mintel occurrence data were available. This made it possible to derive year specific local emissions and year specific PEC values to reflect the temporal decline in TCS use in cosmetics over time and its effect on environmental exposure. Historical market surveys are broadly consistent with a low occurrence pattern concentrated mainly in toothpaste, deodorants, nail products and hand soap, rather than uniform occurrence across all permitted product types (Danish EPA, 2016).

For the refined assessment, local emission to wastewater for each category was calculated as follows:

$$Elocal = \sum_{i=1}^{n} Q_i \times C_i \times F_{occ,i} \times F_{inh,i} \times F_{STP,i}$$

Q_i = daily amount of product used in category i
C_i = TCS concentration in product category i
$F_{occ,i}$ = fraction of products in category i containing TCS
$F_{inh,i}$ = fraction of inhabitants using product category i
$F_{STP,i}$ = fraction released to sewer after use

In the higher tier, the fraction released to sewer was corrected for dermal uptake. Based on the *in vitro* human skin penetration study, reported by Moss and colleagues and summarised in the SCCP opinion on triclosan, 6.3% of the applied TCS dose was considered systemically absorbed or retained from immediate release to wastewater. Therefore, 93.7% of the applied TCS amount was assumed to remain available for release to wastewater after product use, and F_{STP} was set at 0.937 in the refined exposure calculation (Moss et al., 2000; SCCP, 2009). Category specific emissions were then summed to derive the total refined local emission to wastewater, Elocal, which was used as input for EUSES (see **Supplementary Data 3**).

Category specific emissions were summed to derive the total refined

local emission to wastewater, Elocal, which was then used as input for EUSES. In contrast to the Tier 0 calculation, for which the STP distribution was derived using EUSES SimpleTreat, the refined Step 9 assessment used the field-based wastewater treatment mass balance reported by Singer and colleagues (Singer et al., 2002). The fraction of TCS released to receiving surface water after wastewater treatment was set at 6%, corresponding to the mass balance reported by Singer and colleagues, in which 79% of incoming TCS was attributed to biological degradation, 15% to sorption to sludge and 6% to input into receiving surface water. This value was retained as the refined wastewater treatment parameter, because it represents a measured downstream release estimate and is slightly more conservative than the effluent fractions reported in previous studies (Bester, 2003; Stasinakis et al., 2010).

RCRs, defined as the ratio of the refined $PEC_{surface\ water}$ to the PNEC, were calculated against PNEC—NGRA-lowest and PNEC—NGRA-SSD derived in **Step 8**. The resulting NGRA-based risk conclusions were benchmarked against an RCR calculated using a conventional PNEC based on apical ecotoxicity data, to assess whether the NGRA approach reaches a conclusion that is at least as protective as conventional ERA.

Step 10: assessment of the level of confidence and evaluation of potential uncertainties

The uncertainty analysis followed the approach previously described (Dent et al., 2018), adapted to the environmental domain. Principal sources of uncertainty were identified across the assessment steps, covering the read-across substance selection, the biokinetic correction, taxonomic data coverage, and the MoA hypothesis. Each source was evaluated in terms of its likely direction of effect on the risk conclusion and its relative magnitude. A qualitative confidence (high, medium or low) was assigned to the overall risk conclusion, reflecting the weight and consistency of the evidence assembled across Steps 1 to 9 and the degree to which residual uncertainties were addressed by the assessment factors applied at Step 8.

Results

Tier 0: Identification of use scenario and collection of existing data

Step 1: exposure / use scenarios of the target substance

The lower tier aggregate exposure assessment yielded a screening $PEC_{surface\ water}$ of 0.74 μg/L. This value was carried forward for the Tier 0 comparison against the ecoTTC and read across thresholds. As the Tier 0 exit criteria were not met, the exposure assessment was refined in Step 9 using product category specific and year specific market occurrence data.

Step 2: identification of the molecular structure/class of the target and its degradation products

TCS is a chlorinated diphenyl ether with a phenolic hydroxyl group, classified as a phenol-class compound across different profiling tools. The characterisation was extended to known and predicted transformation products, including the known degradation product methyl-triclosan (CAS 4640–01–1) and the ones predicted using the EAWAG-BBD pathway tool: 5-chlorobenzene-1,2,3-triol (CAS 100,859-41–4), 2,4-dichlorophenol (CAS 120–83–2), 4-chlorocatechol (CAS 2138–22–9) and 3,5-dichlorocatechol (CAS 13,673-92–2).

In silico PBT profiling of these transformation products using EPI Suite v.4.11 (US EPA, 2025), ProtoQSAR v.1.0 (ProtoPRED, 2025) and ECOSAR v.2.2 (US EPA, 2022) indicated that, although methyl triclosan exhibits persistence properties, none of the transformation products were concluded to be PBT; they were therefore not considered further in the subsequent steps. All predictions were within the applicability domain, except for the toxicity assessment of methyl triclosan using ECOSAR v.2.2 (see **Supplementary Data 4**).

MoA profiling results are summarised in Table 2. TCS was classified as a narcotic compound (phenols class) across different profiling platforms, giving a consensus narcosis classification with a confidence score of 2; the corresponding ecoTTC is 0.1 μg/L (de Wolf et al., 2005). *In silico* ED profiling identified estrogenic binding, androgen receptor (AR) antagonism and thyroid pathway activity as the most consistent signals across the different tools, with positive predictions for AR binding and inhibition (Benfenati et al., 2013; Danish (Q)SAR Database, 2026) and thyroid receptor beta (TRβ) binding and sodium/iodide symporter (NIS) activity (Danish (Q)SAR Database, 2026). The OECD QSAR Toolbox additionally predicted strong ER binding, indicating mixed endocrine activity across multiple hormonal pathways. These findings are overall consistent with a previous *in silico* and *in vitro* assessment (Kenda et al., 2020), which reported AR antagonist activity, moderate TR binding and weak ER binding for TCS using Endocrine Disruptome and VirtualToxLab. The complete ED profiling outputs across all tools are provided in **Table S3 in Supplementary Data 2**. Overall, given the mixed endocrine profile with weak estrogenic binding alongside stronger AR antagonism and thyroid effects, a conservative approach was adopted using the more protective estrogenic ecoTTC range of 0.0003–0.0092 μg/L (Gross et al., 2010) for the Tier 0 exit comparison.

With the lower tier screening PEC of 0.74 μg/L, the narcosis based ecoTTC of 0.1 μg/L was exceeded. The more conservative endocrine related ecoTTC range of 0.0003–0.0092 μg/L was also exceeded.

Step 3: ecotoxicity and environmental fate data collection and identification of data gaps

The data compilation confirmed that TCS is a well-studied compound with an extensive ecotoxicological and environmental fate dataset. Apical toxicity data were identified across all three standard aquatic taxonomic groups, including chronic and acute endpoints for algae, aquatic invertebrates and fish, as well as data for sediment-dwelling organisms. Physico-chemical properties and environmental fate data confirmed that TCS has low water solubility (6.5 mg/L), high

Table 2
In silico MoA profiling.

In silico tool	Submodels	Results
EnviroTox	ECOSAR classification	Phenols
	US-EPA New Chemical Categories	Phenols (Acute toxicity)
	TEST coded	N
	TEST	Narcosis
	ASTER coded	N
	ASTER	Nonpolar narcosis
	OASIS coded	N
	OASIS	Phenols and Anilines
	Verhaar coded	S
	Actual Verhaar Category	Class 3 (unspecific reactivity)
	4 letter code	NNNS (three schemes in agreement)
	Consensus MOA	**N (narcotic)**
	MOA Confidence score	2
OECD QSAR Toolbox v.4.7	iSafeRat - MechoA 1.2	Polar narcosis
	Acute aquatic toxicity classification by Verhaar (Modified)	Class 3 (unspecific reactivity)
	ECOSAR classification	Phenols
	OASIS	Phenols and Anilines
Overall conclusion:		**Narcosis**

N: Narcotic; S: Specifically acting; NNNS: three of the four classification schemes indicated narcotic (N), one indicated specifically acting (S); MoA: mode of action; ECOSAR: Ecological Structure Activity Relationships; TEST: Toxicity Estimation Software Tool; ASTER: Assessment Tools for the Evaluation of Risk; OASIS: Optimised Approach based on Structural Indices Set; EnviroTox: Environmental Toxicology database and analysis platform.

lipophilicity (log Kow: 4.9), hydrolytic stability (t½ > 1 year), moderate adsorption potential (log Koc: 2.92), and it is inherently but not readily biodegradable (ECHA CHEM, 2026). TCS is detected in surface waters, predominantly downstream of wastewater treatment plant discharges, at concentrations in the range of <LOD to 3.06 μg/L based on records compiled in the NORMAN EMPODAT Database (refer to **Supplementary Data 1**) (Bedoux et al., 2012; Halden and Paull, 2005; NORMAN Association, 2026). ED concerns have been identified for TCS through the ECHA PACT process, with both PBT and ED assessments, which are currently under development (ECHA PACT, 2025).

Several existing PNEC and EQS values for TCS were identified and summarised in **Table S4 of Supplementary Data 2** for reference. These values ranged from the Danish EPA saltwater EQS of 0.005 μg/L (Miljøministeriet, 2010) to 0.843 μg/L from ECHA (ECHA CHEM, 2026), using SSD analysis and an assessment factor (AF) of 1, which reflects a variation in the underlying ecotoxicity datasets, derivation methods and the choice of assessment factors across regulatory bodies. For the purpose of this case study, the PNEC of 0.843 μg/L from the ECHA REACH dossier (ECHA CHEM, 2026) was used for the Step 3 exit comparison. The comparison of this value against the lower tier screening PEC of 0.74 μg/L gives a PEC/PNEC ratio of 0.88. Although this ratio below 1 would typically indicate no concern under conventional risk assessment criteria, the REACH PNEC incorporates vertebrate ecotoxicity data that are excluded from the NGRA framework for the purpose of this case study. Therefore, the assessment proceeded to the next step to identify analogues with vertebrate data, derive PNEC values for the comparison with PEC and evaluate the possibility of exit at Tier 0. All regulatory benchmarks will be used as external reference points for later comparison with NGRA-derived PNEC values.

Step 4: identification and evaluation of potential analogues, collection of read-across data and derivation of PNEC

Diclosan (5-chloro-2-(4-chlorophenoxy)phenol; CAS 3380–30–1) was identified as a suitable analogue (Table 3). Structurally, diclosan shares the same diphenyl ether backbone as TCS, but it presents two chlorine atoms rather than three.

Diclosan shows a relatively high DICE similarity index, and both compounds share the same key functional groups, including aryl halide, ether moiety and phenol. Physico-chemical properties are within a comparable range, with diclosan being slightly more bioavailable than TCS. With respect to structural alerts, the two compounds present the same structural alerts identified by 'acute aquatic toxicity classification by Verhaar (Modified)', 'acute aquatic toxicity MOA by OASIS' and 'aquatic toxicity classification by ECOSAR' profilers. With respect to microbial metabolism, both substances are predicted to undergo aromatic hydroxylation, and their predicted degradation pathways are similar. The PBT profiling indicated a comparable behaviour for both compounds (see **Supplementary Data 4**). Additionally, the two compounds share the same narcotic MoA, due to the chlorinated diphenyl ether substructure, and comparable aquatic toxicity profiles across all profiling systems used. On this basis, diclosan was considered to be a suitable analogue (refer to **Table S5** in **Supplementary Data 2** for details).

For the purpose of this case study, existing *in vivo* vertebrate ecotoxicity data for TCS were deliberately excluded from the Tier 0 read-across-based PNEC derivation, with diclosan being used as the primary source for the vertebrate data component. However, early developmental stage data from vertebrate species (*e.g.* fish embryos and amphibian eleutheroembryos) for TCS were included, as these assays are conducted prior to protected life stages as per the Directive 2010/63/EU, and they are recognised as alternative approaches aligned with the 3Rs (EC, 2012, 2020). Ecotoxicity data from the TCS dossier were used for all the other ecotoxicity endpoints, including invertebrate and algal endpoints. Using the diclosan vertebrate dataset alongside the available TCS algal endpoint (96-h ErC_{10} of 1.46 μg/L), three interim read-across PNECs were derived: 0.0146 μg/L (combined dataset, with AF 100 being applied in the absence of chronic vertebrate data) and 0.021 μg/L (SSD-derived HC_{05} of 0.211 μg/L, Gumbel distribution, best fit by AICc) (see **Fig. S1** in **Supplementary Data 2** for details). A sensitivity analysis excluding *Chironomus riparius* (n = 4) yielded a Weibull-derived HC_{05} of 0.289 μg/L (PNEC: 0.029 μg/L), confirming the robustness of the SSD result. An AF of 10 was applied to both SSD-derived PNECs to account for limited species coverage (n: 4–5). Indeed, ECHA Guidance R.10 recommends AF of 1–5 for SSDs based on ≥10 species covering ≥8 taxonomic groups (ECHA, 2008); therefore, a higher AF was applied given the small size of the dataset. Using the lower tier screening PEC of 0.74 μg/L, all three interim read across PNECs were exceeded. The PEC/PNEC ratios were 50.7 for the most conservative read across PNEC of 0.0146 μg/L, 35.2 for the SSD derived PNEC of 0.021 μg/L, and 25.5 for the sensitivity analysis PNEC of 0.029 μg/L. The lower tier PEC was also above both the narcosis-based ecoTTC and the more conservative endocrine related ecoTTC range. Because Tier 0 did not yield a low concern conclusion under this conservative screening scenario, the assessment proceeded to Tier 1.

Tier 1: Hypothesis formulation for *ab initio* approach

Step 5: bioavailability estimation and QIVIVE factor derivation

The one-compartment model BCF model used here (Krause and Goss, 2020) predicted a BCF value of 257.4 L/kg taking into account the experimentally determined hepatic clearance (Black et al., 2021). From the calculated BCF value, a QIVIVE factor of 0.0039 was derived (see **Supplementary Data 5**) (Mackay et al., 2014).

This correction factor was applied to *in vitro*-derived effect concentrations only. Specifically, ToxCast AC_{50} values, HTTr and HTPP BMD values as well as PubChem bioactivity data were corrected, because these are expressed as nominal concentrations in cell culture medium and do not reflect the external aqueous exposure concentrations. The *in vivo* ecotoxicity values from ECOTOX, EnviroTox, ETOX and NORMAN databases were not corrected, as they represent external measured concentrations and are comparable to PEC on the same scale.

Table 3
Structures of the target substance and the analogue.

	Target substance	Analogue
CAS number	3380–34–5	3380–30–1
Name	Triclosan	5-chloro-2-(4-chlorophenoxy)phenol (Diclosan)
2D Structure	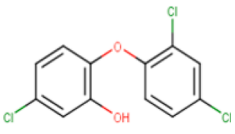	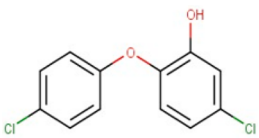
SMILES from PubChem	C1=CC(=C(C=C1Cl)O)OC2=C(C=C(C=C2)Cl)Cl	C1=CC(=CC=C1OC2=C(C=C(C=C2)Cl)O)Cl

Step 6: MoA hypothesis

Data collection and curation: Across all the bioactivity and ecotoxicity database searches for TCS, a total of 12,162 records were retrieved. These records were subsequently screened and curated using predefined inclusion and exclusion criteria (refer to **Table S1** in **Supplementary Data 2**), resulting in a final dataset of 5219 records for analysis (see **Supplementary Data 6**).

The curation steps varied depending on the data source (refer to **Table S1** in **Supplementary Data 2** for details):

- For ToxCast, only the lowest AC_{50} value per assay was retained and inactive hit calls were excluded, reducing the dataset from 870 to 345 records.
- For the PubChem bioassay data, 2508 records were retrieved directly from PubChem, and 2504 records were retrieved via the CompTox Chemicals Dashboard PubChem module. These records were consolidated into a combined pool of 5012. Upon removal of duplicates between the two access routes of records with either missing values, non-standard descriptors or inconclusive results, 16 records were retained.
- For HTTr, 978 records were filtered against a cytotoxicity threshold of 12.051 μM, obtaining a final number of 215 records.
- For HTPP, entries without BMD values were excluded, reducing the number of entries from 4050 to 3829.
- For NORMAN, ECOTOX, ETOX,and EnviroTox, the 1102 records were combined, databases were merged, deduplicated, and filtered to get 190 records.
- CTD and literature searches contributed a further 118 and 506 records, respectively (see **Table S1** in **Supplementary Data 2** for details on each curation step).

The curated integrated TCS hazard dataset of 5219 records covers two broad test types: traditional ecotoxicological studies (269 records) and NAMs (4950 records). The NAM dataset consists of bioactivity data (4508 records) and omics-based data (442 records). The latter further includes transcriptomic (413 records), proteomic (20 records), and metabolomic (9 records) data (see **Supplementary Data 6**). Bioactivity data were primarily derived from ToxCast (345 records), HTPP (3829 records), and supplementary sources (CTD and PubChem), and include effects such as effects on cell phenotype, cellular stress pathways, enzyme and receptor activity, gene expression, receptor binding and protein levels, cell proliferation (refer to **Table S2** in **Supplementary Data 2** for details). Of note, gene expression data appear in both the bioactivity and transcriptomic categories. In the bioactivity dataset, these originate from single-gene reporter assays (ToxCast and CTD), whereas multi-gene HTTr datasets form the transcriptomic category. Ecotoxicological records include population-level and organism-level effects, such as growth, reproduction, mortality and behaviour (refer to **Table S2** in **Supplementary Data 2** for details).

The integrated TCS hazard dataset covers 75 species and test systems assigned to seven taxonomic groups: algae, aquatic invertebrates, terrestrial invertebrates, lower vertebrates, aquatic vertebrates, aves, and mammals. Ecotoxicological data provide the coverage of algae (three species), aquatic invertebrates (including daphnids, molluscs and rotifers), and aquatic vertebrates (mainly fish). Within the NAMs dataset, most records are from mammalian *in vitro* systems (4243 records), with some assays from invertebrate (110 records), fish (111 records) and avian (6 records) cell lines. Together, this coverage includes molecular and cellular responses through to organism-level and population-level endpoints, allowing the comparison of effects across levels of biological organisation and ecological relevance, and supporting both mechanistic interpretation and regulatory risk assessment. The curated datasets formed the basis for the MoA hypothesis formulation including pathway enrichment analysis (KEGG, Reactome and GO) and SSD modelling.

The distribution of effect concentrations across taxonomic groups and effect categories, following curation and QIVIVE correction, is shown in Fig. 2. The plot illustrates the concentration range covered by the integrated TCS hazard dataset, the relative density of data points per taxonomic group, and the separation between *in vitro* QIVIVE-corrected values and *in vivo* ecotoxicity records. Mammalian data points cluster at the lower end of the concentration range for several effect categories. This likely reflects not only the sensitivity of receptor-based assays relative to apical ecotoxicity endpoints, but also the broader representation of mammalian assay systems within the curated integrated TCS hazard dataset. These patterns were therefore used cautiously to inform target prioritisation and the taxonomic scope of the subsequent pathway enrichment analysis, rather than being interpreted as evidence that the lowest mammalian signals necessarily provide the most appropriate hazard anchor.

MoA hypothesis formulation: Following the curation and quality assessment of the integrated TCS hazard dataset including the NAMs data (Step 5), the next step was to characterise the MoA of TCS, by examining the biological processes affected across species and endpoint types. This was approached in two stages: first, a systematic grouping of the curated endpoints into potential MoA pathways based on their underlying biological function; and second, a confirmatory pathway enrichment analysis using the transcriptomic subset of the data. An overview of the potential MoA pathways, species coverage and concentration ranges is provided in Table 4. The pathways are presented below in order of their combined weight of evidence, based on the number of curated endpoints, the diversity of species tested, and the breadth of taxonomic groups represented.

Biological activity characterisation based on the curated NAMs dataset

To characterise the biological activity of TCS across taxa, the curated NAMs dataset was grouped by the underlying biological function of each assay including enzyme activity measurements, receptor-based bioassays, transcriptomic assays, protein-level measurements, metabolomic profiles, and cellular stress markers. This process identified eleven potential biological activity categories including molecular targets and cellular response pathways, as described below.

Energy metabolism and mitochondrial function were the most common across different and distant taxa, with 114 records across 15 species and 11 taxonomic groups at concentrations from 0.043 μg/L (chlorophyll a in *Chlamydomonas reinhardtii*) to 11,582 μg/L (*age-1* and *akt-1* gene expression in *Caenorhabditis elegans*) (Xin et al., 2019; Yoon et al., 2017). Evidence included mitochondrial depolarisation and metabolomic disruption of central carbon metabolites in *Danio rerio*, adenosine triphosphate (ATP) perturbation and altered enzyme activity (lactate dehydrogenase (LDH), creatine kinase (CK), adenosine triphosphatase (ATPase)) in *Daphnia magna*, extensive photosynthesis gene expression changes (photosystem I/II subunits, light-harvesting complex proteins, chlorophyll biosynthesis genes) in *Raphidocelis subcapitata*, chlorophyll perturbation across multiple algal species, energy metabolism pathway gene expression in *Euglena gracilis* and *Chironomus dilutus*, and metabolite-level disruption of central carbon and amino acid metabolites in *C. elegans*. These findings indicate that TCS perturbs cellular energy production across both heterotrophic and autotrophic organisms.

Endocrine receptor-mediated signalling was observed across 17 species and eight taxonomic groups (155 records), with effect concentrations ranging from 0.011 μg/L (*insulin-like growth factor binding protein 1* (*IGFBP1*) gene expression in *Homo sapiens*) to 32,417 μg/L (pregnane X receptor (*PXR)* transcriptional activation in *H. sapiens*) (Forte et al., 2016; Lu and Archer, 2005). AR and ER activity was altered across fish, amphibians, reptiles, birds and mammals through receptor-based bioassays. Additional nuclear receptor activities (PXR, aryl hydrocarbon receptor (AHR), constitutive androstane receptor (CAR), vitamin D receptor (VDR), retinoic acid receptor (RAR), retinoid X receptor (RXR),

(caption on next page)

Fig. 2. Strip plot showing the distribution of effect concentrations for TCS across taxonomic groups and effect categories following data curation and QIVIVE correction (total n = 5219 study records; Mammals n = 4485; Aves n = 6; Lower vertebrates n = 8; Aquatic vertebrates n = 233; Terrestrial invertebrates n = 64; Aquatic invertebrates n = 208; Algae n = 215).
Effect concentrations are expressed as $\log_{10}$(μg/L) on the x-axis. Each data point represents a study record from the curated bioactivity and ecotoxicity dataset assembled in Step 6. Triangles indicate *in vivo* ecotoxicity data retrieved from ECOTOX, EnviroTox, ETOX and NORMAN databases; circles indicate *in vitro* bioactivity values from ToxCast, HTTr, HTPP and PubChem, converted to external aqueous concentration equivalents using the quantitative *in vitro* to *in vivo* extrapolation (QIVIVE) factor derived in Step 5 (Mackay et al., 2014). Horizontal lines indicate the minimum-to-maximum concentration range per effect category within each taxonomic group. Within each taxonomic group, effect categories are ordered by descending median $\log_{10}$ effect concentration, and the number of study records per group is annotated alongside the group label. Blue shading indicates algae; orange shading indicates aquatic invertebrates; purple shading indicates terrestrial invertebrates; green shading indicates aquatic vertebrates; teal shading indicates lower vertebrates; yellow shading indicates aves; white/grey shading indicates mammals. The figure was generated in Python (v.3.12) using matplotlib. QIVIVE: quantitative *in vitro* to *in vivo* extrapolation.

Table 4
Summary of the potential biological pathway categories for TCS.

Biological pathways	Most sensitive endpoint	Most sensitive species	Lowest effect concentration (μg/L)	Effect concentration range (μg/L)
PPAR signalling and lipid/ steroid metabolism	HMGCS2 mRNA expression	*Homo sapiens*	0.007	0.007–1870
Nuclear receptor and endocrine signalling	IGFBP1 gene expression	*Homo sapiens*	0.011	0.011–32,417
Energy metabolism and mitochondrial function	Chlorophyll a concentration	*Chlamydomonas reinhardtii CPCC 12, Chlamydomonas reinhardtii CPCC 243, Asterococcus superbus, Eremosphaera viridis*	0.043	0.043–11,582
Immune signalling	IL-1β and IL-6 protein levels and mRNA expression	*Homo sapiens*	0.056	0.056–3900
Oxidative stress response	SOD, CAT, GPx, and GST activity and ROS protein levels	*Danio rerio*	0.1	0.1–11,582
Xenobiotic metabolism and biotransformation	P-gp efflux functionality	*Danio rerio*	0.1	0.1–11,582
Apoptosis and cell cycle	BAX, CCND1, CDKN1A mRNA and protein levels	*Homo sapiens*	0.113	0.113–1870
Neuronal and cardiac signalling	AChE activity	*Rhamdia quelen*	0.5	0.5–600
Thyroid hormone disruption	Dio III mRNA levels	*Danio rerio*	0.565	0.565–97
Protein homeostasis and ER stress	MATN1 gene expression	*Homo sapiens*	1.13	1.13–11,582
Calcium and ion transport	L-type calcium channel blockade	*Homo sapiens*	2.89	2.89–11,582

farnesoid X receptor (FXR)) were altered in mammalian systems. Altered protein levels of steroidogenic enzymes (Cyp19a1, Cyp11a1, steroidogenic acute regulatory protein (StAR)) in rat and vitellogenin induction in aquatic invertebrates extended the evidence across vertebrate and invertebrate taxa.

Oxidative stress was the most broadly conserved cellular response, observed across 16 species and 13 taxonomic groups (93 records), at concentrations ranging from 0.10 μg/L (reactive oxygen species (ROS) levels and activity of enzymes like superoxide dismutase (SOD), catalase (CAT), glutathione peroxidase (GPx), glutathione S-transferase (GST) in *D. rerio*) to 11,582 μg/L (*GCS-1* gene expression in *C. elegans*) (Table 4) (Parenti et al., 2019; Yoon et al., 2017). Evidence included: (1) altered activity of antioxidant enzymes (SOD, CAT, GPx, GST, ascorbate peroxidase); (2) altered expression of antioxidant defence genes, including *nuclear factor erythroid 2-related factor 2 (Nrf2)* in vertebrates and its functional counterpart *SKN-1* in *C. elegans*; and (3) lipid peroxidation markers (thiobarbituric acid reactive substances (TBARS), malondialdehyde (MDA)) and cytological indicators of genotoxic stress (micronucleated cells in *Dreissena polymorpha*). The breadth of this response across algae, diatoms, rotifers, nematodes, crustaceans, copepods, insects, molluscs, fish and mammals indicates that oxidative stress is a primary and widely conserved biological response to TCS.

Apoptosis and cell cycle perturbation was observed across nine species and six taxonomic groups (175 records) at concentrations from 0.11 μg/L (*BCL2-associated X* protein (*BAX*) mRNA expression and protein levels in *H. sapiens*) to 1870 μg/L (*MAPK interacting serine/threonine kinase 2b* (*MKNK2B*) gene expression in *D. rerio*) (Haggard et al., 2016; Kim et al., 2014). Key evidence included 1) protein-level changes in BAX, cyclin D1 (CCND1) and cyclin-dependent kinase inhibitor 1A (CDKN1A/p21) in human cells; 2) caspase-3/7 activity, caspase-3/7 activity and altered expression of core apoptotic genes (*Bax, Bcl-2, p53, caspase-9, caspase-6, fasl, perp*) in *D. rerio*; 3) cleaved poly (ADP-ribose) polymerase (PARP) expression in *D. magna*; and 4) cell cycle gene alteration in *Raphidocelis subcapitata*.

Alterations in peroxisome proliferator-activated receptor (PPAR) signalling and lipid/steroid metabolism were observed across 12 species and nine taxonomic groups (76 records) at concentrations from 0.007 μg/L (*3-hydroxy-3-methylglutaryl-CoA synthase 2* (*HMGCS2*) mRNA in *H. sapiens*) to 1870 μg/L (*retinol-binding protein 2b* (*RBP2B)* gene expression in *D. rerio*) (Haggard et al., 2016; US EPA, 2026b). Evidence included metabolite-level disruption (stearic acid, L-proline, cholesterol and phospholipids) in aquatic species, fatty acid synthase (FASN) enzyme inhibition in birds, transcriptomic regulation of lipid biosynthesis genes (*FASN, sterol regulatory element-binding protein* (*SREBP*), *carnitine palmitoyltransferase 1 (CPT1), acyl-CoA oxidase 1* (*ACOX1*), *HMGCS2*), and PPARγ/CCAAT/enhancer-binding protein alpha (C/EBPα)-mediated adipogenic signalling in mammals. Lipid and pigment perturbation in diatoms and algae extended this response to primary producers.

Xenobiotic metabolism and biotransformation were observed across 14 species and seven taxonomic groups (63 records), with effect concentrations ranging from 0.10 μg/L (P-glycoprotein (P-gp) efflux in *D. rerio*) to 11,582 μg/L (*peroxisomal membrane protein 3* (*PMP-3*) gene expression in *C. elegans*) (Parenti et al., 2019; Yoon et al., 2017). Evidence included modulation of P-gp efflux activity, modulation of cytochrome P450 (CYP) enzyme activity across multiple isoforms, and transcriptional modulation of CYP, *ATP-binding cassette (ABC) transporter, sulfotransferase and UDP-glucuronosyltransferase (UGT)* genes in

algae, rotifers, nematodes, copepods, midges, fish and mammals. These observations indicate a broad perturbation of Phase I and Phase II biotransformation pathways.

Immune signalling was observed across six species and four taxonomic groups (145 records), with effect concentrations ranging from 0.056 μg/L (interleukin-1 beta (IL-1β) levels in *H. sapiens*) to 3900 μg/L (*tumor necrosis factor alpha* (*TNF-α)* gene expression in *H. sapiens*) (Marshall et al., 2015; Wilburn et al., 2024). Evidence included altered cytokines at gene expression and protein levels (IL-1β, interleukin-6 (IL-6), TNF-α, transforming growth factor beta 1 (TGF-β1)) and inducible nitric oxide synthase (iNOS) protein expression, prostaglandin-endoperoxide synthase 2/cyclooxygenase-2 (PTGS2/COX-2) enzymatic activity, and a broad panel of inflammation-associated protein markers in mammalian systems. In non-mammalian species, immune cell count alterations and immune-related gene expression were observed in *D. rerio*, and *gamma-interferon-inducible lysosomal thiol reductase* (*GILT*) gene expression was altered in *C. dilutus*.

Neuronal and cardiac signalling were observed across eight species and four taxonomic groups (119 records) at concentrations from 0.50 μg/L (acetylcholinesterase (AChE) activity in *Rhamdia quelen*) to 600 μg/L (*ELAV-like RNA-binding protein 3* (*Elavl3*), *glial fibrillary acidic protein* (*gfap*), *myelin basic protein (mbp), neurogenin 1 (ngn1), neuroD (nrd), α1-Tubulin,* and *growth associated protein 43* (*gap43)* gene expression in *D. rerio*) (Gomes et al., 2021; Kim et al., 2018). Functional evidence included spontaneous neural activity and neural network perturbation in *R. norvegicus* cortical cultures, binding to different neurotransmitter transporters and receptors in mammalian systems, and decreased neurodevelopmental marker gene expression (*gfap, oligodendrocyte transcription factor 2* (*olig2*), *ngn1, brain-derived neurotrophic factor* (*bdnf*), *nestin*, mbp) and cardiac gene expression (*GATA binding protein 4* (*gata4*), *NK2 homeobox 5* (*Nkx2.5*), *natriuretic peptide A* (*Nppa*)) in *D. rerio*. Neurotrophin and N^6-methyladenosine (m^6A) pathway gene expression in *D. magna* extended the evidence to aquatic invertebrates.

Protein homeostasis and endoplasmic reticulum (ER) stress were observed across seven species and seven taxonomic groups (58 entries) at concentrations from 1.13 μg/L (*matrilin 1* (*MATN1)* gene expression in *H. sapiens*) to 11,582 μg/L *RNA binding domain protein 1* (*rbd-1)* gene expression in *C. elegans*) (Du et al., 2018; Yoon et al., 2017). Heat shock protein gene induction (Hsp10–90 family members) was observed in *C. elegans, Brachionus koreanus, Chironomus riparius* and *D. rerio*, while altered expression of unfolded protein response genes (*X-box binding protein 1 (XBP1), activating transcription factor 4 (ATF4), activating transcription factor 6 (ATF6), DNA damage-inducible transcript 3 (DDIT3))* was observed in *H. sapiens* and increased C/EBP homologous protein (CHOP) protein levels were observed in *D. magna*.

Thyroid hormone disruption was observed across five species and three taxonomic groups (24 entries) at concentrations from 0.56 μg/L (*iodothyronine deiodinase type III (Dio III) and transthyretin (Ttr*) mRNA in *D. rerio*) to 97 μg/L (Dio III enzymatic activity in *H. sapiens*) (US EPA, 2026b; Zhou et al., 2017). Evidence converged across three levels: gene expression (*(Dio I–III, Ttr, THRα, THRβ mRNA)*, receptor activity (TRα, TRβ in fish, reptiles and bovines), and enzyme inhibition (thyroperoxidase (TPO), iodothyronine deiodinase, iodotyrosine deiodinase (IYD)). This multi-level convergence indicates that thyroid hormone signalling is a consistent target of TCS across vertebrate taxa.

Calcium and ion transport perturbation was observed across four species and four taxonomic groups (15 entries) at concentrations from 2.9 μg/L (L-type calcium channel blockade in *H. sapiens*) to 11,582 μg/L (*voltage-gated* L-*type calcium channel subunit* (*egl-19)* gene expression in *C. elegans*) (US EPA, 2026a; Yoon et al., 2017). Evidence included L-type calcium channel blockade and ion channel gene expression signatures in humans, intracellular calcium content changes in *D. magna*, and *egl-19* gene expression in *C. elegans*. Although this pathway had fewer observations (n = 15), the convergence of transcriptomic and functional evidence across mammalians and invertebrates supports calcium and ion transport as a component of TCS bioactivity.

Pathway enrichment analysis

To provide an independent mechanistic confirmation of the MoA categories identified from the curated bioactivity dataset, biological pathway enrichment analysis was conducted using three complementary databases: KEGG, Reactome and GO. The analysis was performed separately for the three species with sufficient gene-level representation in the dataset: *Homo sapiens, Danio rerio* and *Caenorhabditis elegans*. For each species, differentially expressed genes were mapped to curated pathway and ontology databases, and statistically enriched terms (adjusted p-value < 0.05) were identified. Detailed enrichment statistics for all three databases and species are provided in **Supplementary Data 7** and **Figs. S2–S4 in Supplementary Data 2**.

The comparison across the three species revealed a substantial overlap as well as distinct species-specific signatures. To facilitate cross-species comparison, significantly enriched terms were grouped into six macro-pathway categories based on the biological function: lipid metabolism (including steroid biosynthesis), nuclear receptor and hormone signalling, energy metabolism and mitochondrial function, xenobiotic metabolism and biotransformation, calcium and ion transport, and neuronal and cardiac signalling (see Fig. 3). These species-specific patterns should, however, be interpreted in the context of differences in dataset composition, assay coverage, and gene representation across species, particularly the broader receptor- and signalling-focused assay coverage available for *Homo sapiens*. Five of these six categories showed cross-species enrichment across at least two of the three species: (1) lipid and steroid metabolism was enriched in all three species (steroid biosynthesis, fatty acid metabolism and PPAR signalling in *Danio rerio*; PPARα-activated gene expression and lipid metabolism-related signalling in *Homo sapiens*; and lipid transporter activity and lipid transport in *C. elegans*); (2) xenobiotic metabolism and biotransformation were similarly conserved, with cytochrome P450-mediated metabolism and biological oxidations enriched across all three species by Reactome, and reactive oxygen species metabolic process and oxidative stress response terms additionally enriched in *H. sapiens* and *C. elegans* by GO; (3) calcium and ion transport pathways were enriched across all three species, encompassing ion channel activity, transmembrane ion transport and ion homeostasis processes; (4) nuclear receptor and hormone signalling was strongly enriched in *H. sapiens* and *D. rerio*, including nuclear receptor SUMOylation and ligand-activated transcription, and represented to a lesser extent in *C. elegans*, where phosphatidylinositol-4,5-bisphosphate 3-kinase/protein kinase B (PI3K/AKT) and mechanistic target of rapamycin (mTOR) signalling were more prominent features; (5) neuronal and cardiac signalling was most prominent in *H. sapiens*, reflecting the broad receptor coverage of the ToxCast assay platforms, though ion channel and synaptic signalling terms were also enriched in *D. rerio* and *C. elegans*; (6) energy metabolism was the only category not conserved across all three species — most prominent in *D. rerio* (oxidative phosphorylation, tricarboxylic acid cycle and glycolysis) and enriched to a lesser extent in *H. sapiens*, but not significantly enriched in *C. elegans*. Apoptotic signalling was also common to *D. rerio* and *H. sapiens*, and protein homeostasis via endoplasmic reticulum chaperones was most prominently enriched in *C. elegans*.

Identification of targets with the lowest effect concentration

The lowest effect concentrations per taxonomic group were identified across the complete curated dataset, including gene expression, biochemical, receptor-based, and omics bioactivity data (see Fig. 4 and **Table S6** in **Supplementary Data 2**).

In algae, the most sensitive endpoint was chlorophyll a and b content in *Chlamydomonas reinhardtii, Asterococcus superbus* and *Eremosphaera viridis*, which was significantly decreased at 0.043 μg/L, consistent with

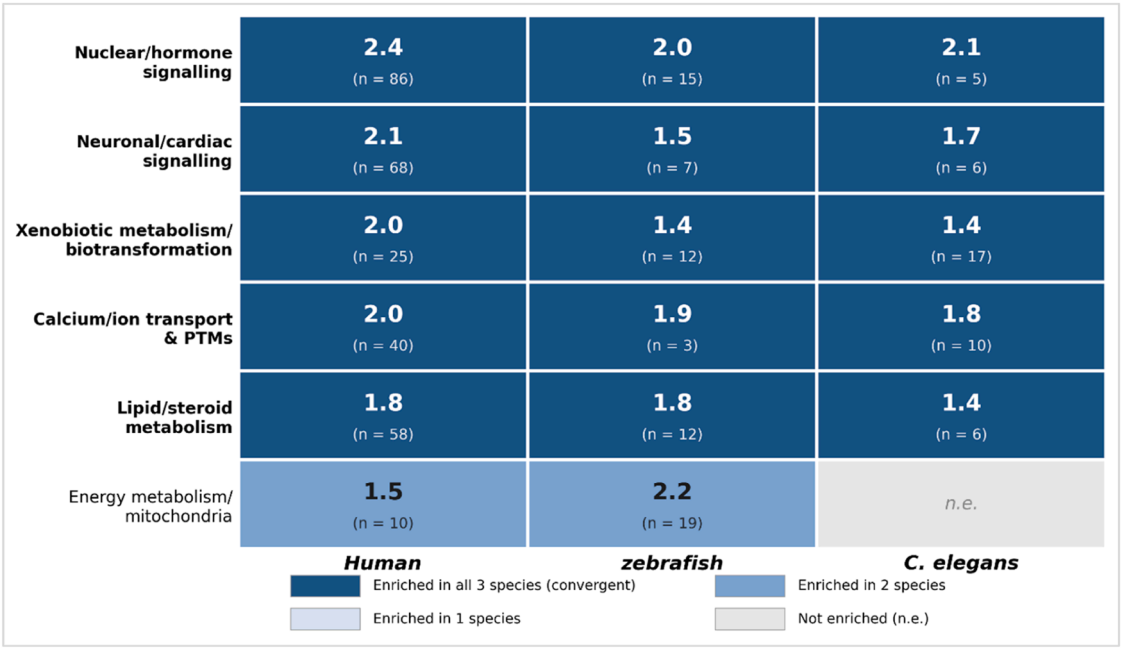

Fig. 3. Colour-coded matrix illustrating pathway enrichment across three species (Homo sapiens, Danio rerio and Caenorhabditis elegans) for TCS, based on over-representation analysis (ORA) of KEGG, REACTOME and GO (Biological Process, Cellular Component, Molecular Function) databases.
All cells shown represent significantly enriched terms (FDR-adjusted p-value < 0.05); statistical significance is therefore a shared baseline across the figure, and the visualisation highlights how that significance is distributed across species rather than ranking individual p-values. Significantly, enriched terms were grouped into six macro-pathway categories defined by biological theme. Each cell displays two values: the upper, bold number is the 25th-percentile of $-\log_{10}$(adjusted p-value), across the enriched terms in that category — summarising the distribution of significance rather than a single most-enriched outlier — and the lower value, "(n = …)", indicates the total count of significantly enriched terms mapped to that category for that species. Cell colour encodes the number of species in which the category is enriched: deep slate blue, all three species; mid blue, two species; pale blue, one species; light grey, no significantly enriched terms in that species ("n.e."). Rows are ordered by the number of cells with $-\log_{10}$ p ≥ 2 (descending), then by maximum $-\log_{10}$ p within tier; categories containing a non-enriched cell appear at the bottom. Multi-category terms (n = 10) were disambiguated by biological context (*e.g.*, "GABA-gated chloride ion channel activity" was assigned to neuronal/ cardiac signalling rather than calcium/ion transport). ORA was performed using clusterProfiler (v.4.10.1) and ReactomePA (v.1.46.0) in R (v.4.3.3) with Benjamini–Hochberg correction (see **Supplementary Data 7**). Human: 195 input genes; Zebrafish: 119 input genes; C. elegans: 35 input genes. Figure generated using Python (matplotlib v.3.10).

photosynthesis inhibition (Xin et al., 2019). This was followed by decreased growth rate based on cell concentration in *Navicula pelliculosa* at 0.10 µg/L (ECHA CHEM, 2026) and decreased growth inhibition based on biomass in *Raphidocelis subcapitata* at 0.20 µg/L (Yang et al., 2008).

In aquatic invertebrates, altered reproduction in *Daphnia magna* was the most sensitive endpoint at 0.34 µg/L (EnviroTox, 2026). At 0.60 µg/L, SOD activity was increased and vitellogenin (VTG) levels were decreased in *Ruditapes philippinarum* (males), indicating concurrent oxidative stress and endocrine disruption responses at the same concentration (Matozzo et al., 2012). Altered reproduction in *Ceriodaphnia dubia* was observed at 4 µg/L (NICNAS, 2009).

In aquatic vertebrates, the lowest effect concentrations were derived from studies with fish embryos. In *Danio rerio* embryos, a panel of oxidative stress and detoxification biomarkers were all significantly increased at 0.10 µg/L: SOD, CAT, GPx, and GST activities were increased, and P-gp efflux functionality was perturbed, consistent with the activation of cellular defence mechanisms (Parenti et al., 2019). Metabolomic targets, stearic acid and L-proline, were also decreased at 0.10 µg/L in the same embryo model (Fu et al., 2019). In *Rhamdia quelen* embryos, both AChE and SOD activities were significantly increased at 0.50 µg/L (Gomes et al., 2021).

In aves, AR antagonistic activity - measured via a chimeric nuclear receptor transactivation assay using *gallus*-derived receptors expressed in human HepG2 cells - was detected at 3.94 µg/L (Houck et al., 2021). Estrogen receptor alpha (ERα) agonistic activity was detected via the same assay system at 8.62 µg/L (Houck et al., 2021). FASN activity was significantly inhibited (decreased) in *An anser domesticus* liver enzyme system at 11.3 µg/L (Abramson, 2011). Cell viability, based on ATP content, was decreased in the *gallus* DT40 cell line at 14.5 µg/L (US EPA, 2026b).

In mammals, the nominally lowest effect concentration in the dataset was recorded for increased *HMGCS2* mRNA expression in primary human hepatocytes at 0.007 µg/L (US EPA, 2026b), within the lipid metabolism and PPAR signalling category. The next most sensitive endpoint was increased (upregulated) IGFBP1 expression in primary human endometrial stromal cells at 0.011 µg/L (Forte et al., 2016), although dose–response analysis was limited by the concentration spacing in the original study. Both mRNA expression and protein levels of pro-inflammatory cytokines IL-1β and IL-6 were significantly increased in peripheral blood mononuclear cells (PBMCs) at 0.056 µg/L (Wilburn et al., 2024).

Across the dataset, the lowest mammalian *in vitro* effect concentration was 0.007 µg/L for increased *HMGCS2* mRNA expression in primary human hepatocytes, while the lowest effect concentration among ecotoxicologically relevant species was 0.043 µg/L for chlorophyll a and b content in freshwater green algae. Both values are reported here as the lowest effect concentrations from the mammalian *in vitro* and environmental species datasets, respectively. The selection of a single candidate ePoD draws on three additional criteria: mechanistic specificity (the molecular target is causally linked to a defined mode of action), cross-species sequence conservation (sufficient to support extrapolation from the species for which the assay has been conducted to environmentally relevant taxa), and consistency with pathway-level evidence (the target maps to a pathway category that is enriched in the curated bioactivity datasets). Mechanistic specificity is supported by the

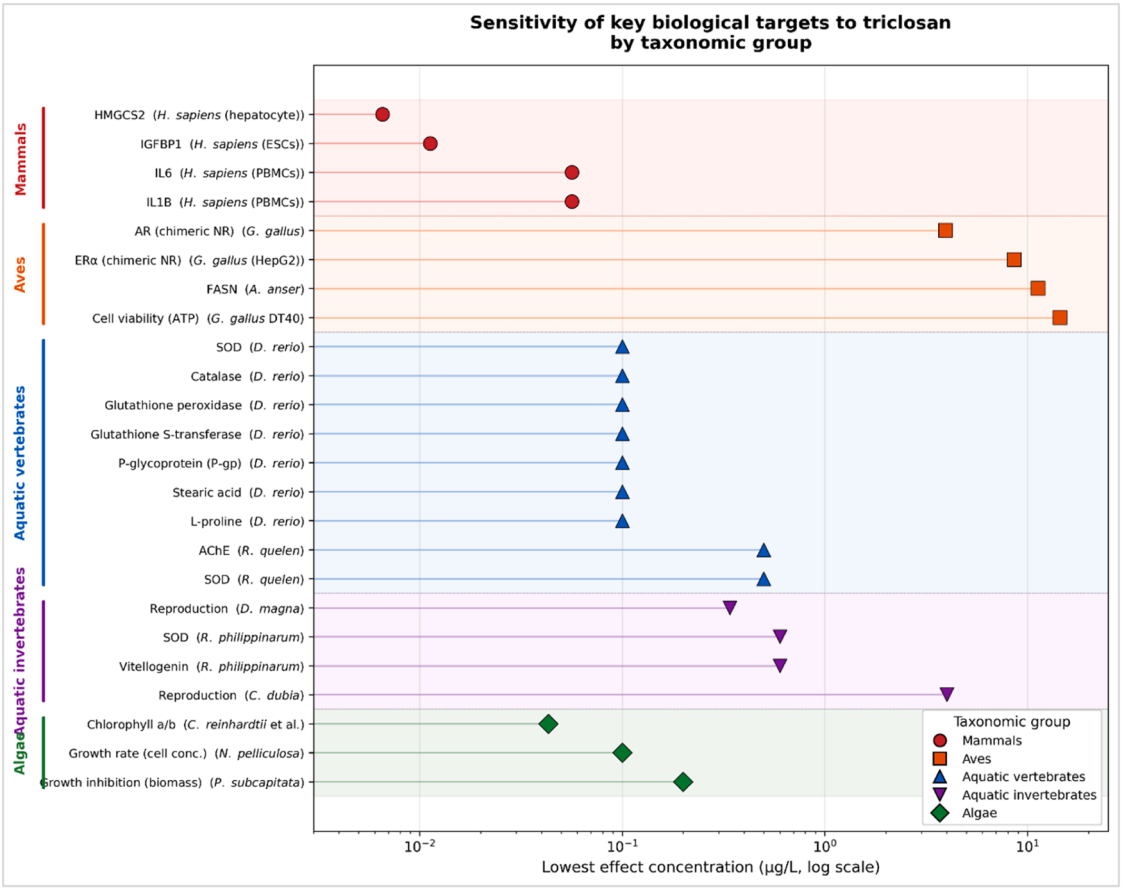

Fig. 4. Lollipop plot showing the lowest effect concentrations (µg/L, log scale) of key biological targets responsive to TCS, grouped by species group. Each point represents the lowest reported effect concentration for a specific biomarker or endpoint in a given test organism, with the horizontal stem indicating its position relative to the concentration axis. Biomarkers are listed on the y-axis with the test species in parentheses; species groups are indicated by coloured brackets on the left margin and by marker shape. Effect concentrations range from 0.007 µg/L (HMGCS2, human hepatocyte cell line) to 14.5 µg/L (cell viability, G. gallus DT40). Figure generated using Python (matplotlib v.3.10).

bioactivity characterisation presented above; cross-species sequence conservation by the SeqAPASS analysis (see subsequent section); and consistency with the broader weight of evidence by the pathway enrichment analysis and the correlation with apical endpoints (see subsequent section). These criteria are evaluated in the following sections and integrated into the final ePoD derivation in Step 8.

Cross-species sequence conservation

To evaluate whether the biological targets identified at the lower end of the effect concentration spectrum are conserved across ecologically relevant species, SeqAPASS analysis was conducted at Level 1 (full amino acid sequence similarity) and Level 2 (functional domain conservation) for all biomarkers with low QIVIVE-corrected effect concentrations (De Roy et al., 2022; LaLone et al., 2018, 2016; Suri et al., 2025). In case the similarity value of Level 2 is higher than the one of Level 1, this indicates that the functional domain is under stronger evolutionary selection pressure than the full protein sequence, thus increasing confidence in cross-species conservation. The selected targets are involved in pathways, which include oxidative stress, xenobiotic metabolism and biotransformation (SOD, CAT, GPx, GST and ATP-binding cassette sub-family B member 1 (ABCB1)), PPAR signalling and lipid/steroid metabolism (PPARγ, HMGCS2, IGFBP1, ACOX2 and VTG), nuclear/hormone signalling (AR, ERα, TRα, TRβ, basic transcription element-binding (BTEB) and thyroid hormone responsive spot 14 beta (THRSPB)), apoptosis and cell cycle (BAX, CCND1, CDKN1A and proliferating cell nuclear antigen (PCNA)), and neuronal/cardiac signalling (AChE). The SeqAPASS results are summarised below, with the complete set of data for Level 1 and Level 2 being provided in Fig. 5 and Table 5. Also refer to **Supplementary Data 8** for detailed analysis.

The SeqAPASS analysis indicates that the majority of the targets at the lower end of the effect concentration spectrum are well conserved across vertebrates at both Level 1 and Level 2. The degree of conservation in invertebrates was variable depending on the target: for SOD, CAT, PCNA and HMGCS2 the similarity value was higher than the threshold of 50% in *D. magna* at both levels, while for the other targets the degree of conservation was low. Functional domain conservation of ERα, AR, PPARγ, TRα and TRβ across vertebrates was generally high, although with some variations depending on the specific domain assessed. Overall, these findings support the biological plausibility of nuclear receptor– and endocrine-mediated effects of TCS across vertebrate species. For HMGCS2, the biomarker associated with the lowest effect concentration in the assessment, the SeqAPASS data confirm that the protein is conserved at both Level 1 and Level 2 across all vertebrates and in *D. magna*, supporting the selection of this target for the derivation of the candidate ePoD in Step 8.

Overall, these findings demonstrate that the biological targets underlying TCS bioactivity are sufficiently conserved to support the use of NAM-derived effect data from one species for the hazard characterisation across ecotoxicologically relevant taxa within the NGRA framework.

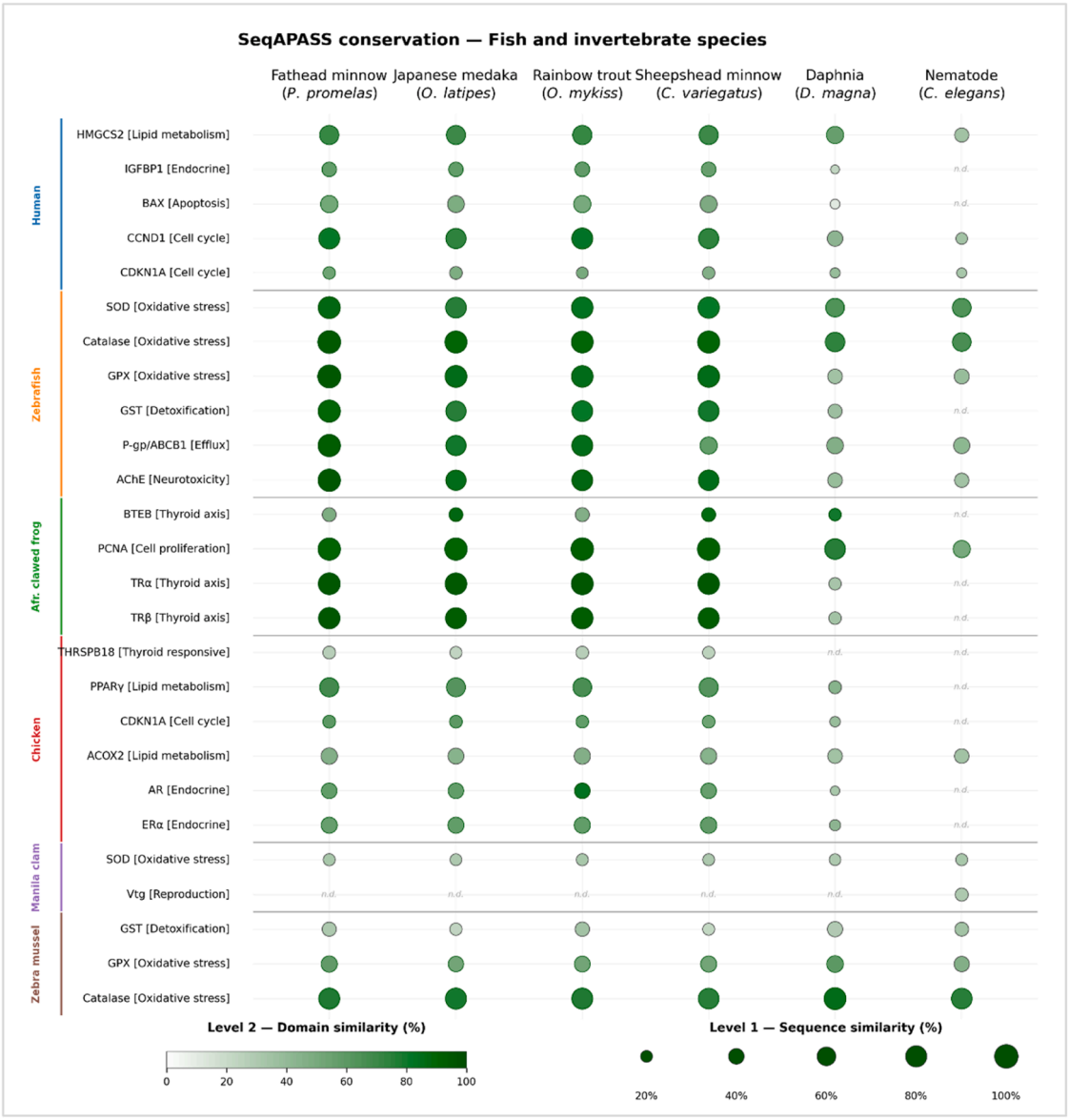

Fig. 5. SeqAPASS conservation analysis for TCS-responsive biomarkers across fish and invertebrate species.
Dot size represents Level 1 similarity (%), based on full-length primary amino acid sequence alignment between the reference and target species. Dot colour intensity represents Level 2 similarity (%), based on the conservation of the functional domain(s). Biomarkers (rows) are grouped by the reference species from which the molecular target was characterised: Human (H. sapiens), Zebrafish (D. rerio), African clawed frog (X. laevis), Chicken (G. gallus), Manila clam (R. philippinarum), and Zebra mussel (D. polymorpha). Target species (columns) include four regulatory fish species — Fathead minnow (P. promelas), Japanese medaka (O. latipes), Rainbow trout (O. mykiss), and Sheepshead minnow (C. variegatus) — and two invertebrates — D. magna and C. elegans. n.d. indicates that no comparable protein sequence was identified in the SeqAPASS database for that species–biomarker combination.

Correlation with apical endpoints as further confirmatory evidence

To assess whether the MoA pathways identified from the curated bioactivity dataset translate into organism-level adverse outcomes, the eleven pathway categories were mapped to apical endpoints from the ecotoxicological dataset (excluding NAM-derived data), comprising 269 records across 50 species. The endpoints included mortality, reproduction, population/growth, development, physiology and behaviour. Each apical endpoint was linked to its most mechanistically relevant MoA pathway(s), yielding 618 MoA–apical associations. The resulting mapping supported biologically coherent relationships between the MoA pathways and the apical effects: energy metabolism and oxidative stress pathways were predominantly associated with population/growth and mortality endpoints; endocrine signalling, PPAR-mediated lipid metabolism, and thyroid hormone disruption mapped primarily to reproduction and development; and neuronal and cardiac signalling corresponded to behavioural and physiological outcomes (Fig. 6**A**).

Furthermore, the lowest bioactivity effect concentrations for all pathway categories were below the 10th percentile (P10) of apical effect concentrations across all endpoint categories (Fig. 6**B**), indicating that molecular perturbations are consistently detected at concentrations lower than those eliciting organism-level adverse effects. This concentration relationship provides additional support to the fact that the MoA characterisation captures biologically relevant pathways linked to the adverse outcomes observed in the ecotoxicological dataset. Because the lowest MoA bioactivity values fell below the 10th percentile of apical effect concentrations across all pathway categories, an ePoD based on an integrated TCS hazard dataset including NAMs would lie below the concentration range at which *in vivo* apical effects are reported, supporting the use of NAMs as a protective basis for environmental hazard

Table 5
Overview of the degree of conservation of TCS bioactivity targets and their relevance to the environmental hazard assessment, using SeqAPASS (Level 1 and Level 2) analysis.

Biological pathway	Targets assessed	Reference species	Vertebrate conservation (Level 1: full sequence)	Vertebrate conservation (Level 2: functional domain(s))	Invertebrate conservation (Level 1: full sequence)	Invertebrate conservation (Level 2: functional domain)	Key conclusions
Oxidative stress / xenobiotic metabolism and biotransformation	SOD	*Danio rerio*	Fish: 76–87% Amphibians: 65% Birds: 66% Mammals: 71–75%	Fish: 75–87% Amphibians: 66% Birds: 67% Mammals: 71–75%	*D. magna*: 61% *C. elegans*: 61%	*D. magna*: 65% *C. elegans*: 64%	SOD (*Danio rerio*) was well conserved across vertebrates and invertebrates at both levels, with similarity values in the same range for both Level 1 and Level 2.
	CAT	*Danio rerio*	Fish: 85–93% Amphibians: 80% Birds: 79% Mammals: 80–82%	Fish: 89–94% Amphibians: 83% Birds: 82% Mammals: 82–85%	*D. magna:* 67% *C. elegans*: 60%	*D. magna*: 73% *C. elegans*: 66%	CAT (*Danio rerio*) was highly conserved across all taxa including invertebrates, with the similarity value of Level 2 consistently higher than the one of Level 1.
	GPx	*Danio rerio*	Fish: 84–95% Amphibians: 68% Birds: 67% Mammals: 73%	Fish: 85–94% Amphibians: 69% Birds: 68% Mammals: 75%	*D. magna*: 34% *C. elegans*: 36%	*D. magna*: 35% *C. elegans*: 38%	GPx (*Danio rerio*) was well conserved across vertebrates but showed low conservation in invertebrates for both Level 1 and Level 2.
	GST	*Danio rerio*	Fish: 73–89% Amphibians: 66% Birds: 69% Mammals: 66%	Fish: 76–90% Amphibians: 70% Birds: 73% Mammals: 70–71%	*D. magna*: 31% *C. elegans*: -	*D. magna*: 37% *C. elegans*: -	GST (*Danio rerio*) was well conserved across vertebrates with the similarity value of Level 2 higher than the one of Level 1; it presented a low degree of conservation in *D. magna*.
	ABCB1	*Danio rerio*	Fish: 51–90% Amphibians: 64% Birds: 64% Mammals: 64–65%	Fish: 57–94% Amphibians: 69–73% Birds: 44–70% Mammals: 71–76%	*D. magna:* 46% *C. elegans:* 43%	*D. magna*: 37–57% *C. elegans*: 36–47%	ABCB1 (*Danio rerio*) was highly conserved across vertebrates while it presented a lower degree of similarity in *D. magna*.
PPAR signalling and lipid/steroid metabolism	PPARγ	*gallus*	Fish: 61–67% Amphibians: 83% Birds: 100% Mammals: 93%	Fish: 23–96% Amphibians: 64–98% Birds: 98–100% Mammals: 80–100%	*D. magna:* 25% *C. elegans:* –	*D. magna* 21–68% *C. elegans:* -	PPARγ (*gallus*) was highly conserved across vertebrates at both Level 1 and Level 2, with the similarity value of Level 2 being consistently higher than the one of Level 1 across all taxa assessed. For *D. magna*, Level 1 conservation was low, but Level 2 conservation was relatively high (68%), suggesting that the functional is highly conserved across taxa, although the conservation of the primary sequence is low.
	HMGCS2	*Homo sapiens*	Fish: 64–65% Amphibians: 65% Birds: 70% Mammals: 91%	Fish: 71% Amphibians: 72% Birds: 76% Mammals: 93%	*D. magna:* 51% *C. elegans:* 32%	*D. magna:* 56% *C. elegans:* 35%	HMGCS2 (*Homo sapiens*) showed the highest conservation profile among the lipid metabolism targets. The similarity value of Level 1 was higher than the threshold of 50% across all vertebrate taxa and in *D. magna*. The similarity value of Level 2 was consistently higher in all vertebrates and *D. magna*.
	IGFBP1	*Homo sapiens*	Fish: 34–35% Amphibians: 46% Birds: 46% Mammals: 70%	Fish: 54–62% Amphibians: 59–71% Birds: 53–74% Mammals: 83–86%	*D. magna:* 8% *C. elegans:* –	*D. magna:* 23% *C. elegans:* –	IGFBP1 (*Homo sapiens*) showed a low degree of conservation for Level 1 in fish, amphibians and birds, the similarity value of Level 2 was substantially higher across all vertebrate taxa. The degree of conservation in *D. magna* was low.
	ACOX2	*Gallus gallus*	Fish: 42–45% Amphibians: 60% Birds: 96% Mammals: 56–59%	Fish: 44–47% Amphibians: 62% Birds: 96% Mammals: 57–60%	*D. magna:* 35% *C. elegans:* 33%	*D. magna:* 35% *C. elegans:* 34%	ACOX2 (*gallus*) was conserved in amphibians, birds and mammals but not in fish and *D. magna*.
Nuclear/hormone signalling	ERα	*Gallus gallus*	Fish: 42–44% Amphibians: 75%	Fish: 10–96% Amphibians: 30–98%	*D. magna:* 17% *C. elegans:* –	*D. magna:* 19–65% *C. elegans:* –	ERα (*gallus*) was shown to be conserved in amphibians, birds and mammals, but not in fish and *D. magna*, with the similarity

(*continued on next page*)

Table 5 (*continued*)

Biological pathway	Targets assessed	Reference species	Vertebrate conservation (Level 1: full sequence)	Vertebrate conservation (Level 2: functional domain(s))	Invertebrate conservation (Level 1: full sequence)	Invertebrate conservation (Level 2: functional domain)	Key conclusions
			Birds: 99% Mammals: 77–78%	Birds: 98–100% Mammals: 29–100%			values of Level 2 substantially higher than the ones of Level 1 across all vertebrates.
	AR	*Danio rerio*	Fish: 41–79% Amphibians: 32% Birds: 31% Mammals: 32%	Fish: 86–99% Amphibians: 71–94% Birds: 70–93% Mammals: 73–94%	*D. magna:* 9% *C. elegans:* –	*D. magna:* 15–50% *C. elegans:* –	AR showed a low degree of conservation for Level 1 in amphibians, birds and mammals, while it substantially increased for Level 2 across all vertebrates. For *D. magna* the degree of conservation was low for Level 1 and increased for Level 2, indicating a partial conservation at the functional domain level
	TRα	*Xenopus laevis*	Fish: 82–87% Birds: 87% Mammals: 87%	Fish: 92–98% Birds: 96–97% Mammals: 94–95%	*D. magna:* 23% *C. elegans:* –	*D. magna:* 24–43% *C. elegans:* –	TRα (*Xenopus laevis*) was highly conserved across vertebrates at both levels, with the similarity value of Level 2 being substantially higher than the one of Level 1. For *D. magna*, the degree of conservation was low.
	TRβ	*Xenopus laevis*	Fish: 78–82% Birds: 83% Mammals: 81–82%	Fish: 90–96% Birds: 97% Mammals: 95–97%	*D. magna:* 23% *C. elegans:* –	*D. magna:* 21–46% *C. elegans:* –	TRβ (*Xenopus laevis*) was highly conserved at both levels, with the similarity value of Level 2 being substantially higher than the one of Level 1. For *D. magna*, the degree of conservation was low.
	BTEB	*Xenopus laevis*	Fish: 30–31% Birds: 43% Mammals: 51%	Fish: 6–88% Birds: 100% Mammals: 27–100%	*D. magna:* 24% *C. elegans:* –	*D. magna:* 80% *C. elegans:* –	BTEB (*Xenopus laevis*) was conserved in mammals, while it showed a low degree of conservation for Level 1 in fish and birds as well as in *D. magna*, with the similarity value of Level 2 being significantly higher across vertebrates and notably in *D. magna*.
	THRSPB18	*Gallus gallus*	Fish: 21–25% Amphibians: 28% Birds: 76% Mammals: 22–23%	Fish: 23–27% Amphibians: 31% Birds: 74% Mammals: 24–25%	*D. magna:* – *C. elegans:* –	*D. magna:* – *C. elegans:* –	THRSPB18 (*gallus*) was poorly conserved at both levels across most taxa.
	VTG	*Ruditapes philippinarum*	X. laevis: 20% D. rerio: 20%	X. laevis: 22% D. rerio: 25%	*D. magna:* – *C. elegans*: 25%	*D. magna:* – *C. elegans*: 30%	VTG (*R. philippinarum*) showed low conservation at both levels. Data for only three comparison species. Should be considered species-specific.
Apoptosis and cell cycle	BAX	*Homo sapiens*	Fish: 48–52% Amphibians: 61% Birds 20% Mammals: 88–92%	Fish: 49–53% Amphibians: 62% Birds: 19% Mammals: 90–92%	*D. magna:* 11% *C. elegans:* –	*D. magna:* 11% *C. elegans:* –	BAX (*Homo sapiens*) was well conserved was conserved in fish, amphibians and mammals but poorly conserved in birds at both levels. and the degree of conservation in *D. magna* conservation was very low
	CCND1	*Homo sapiens*	Fish: 72–79% Amphibians: 78% Birds: 87% Mammals: 89%	Fish: 65–88% Amphibians: 81–84% Birds: 86–95% Mammals: 93–98%	*D. magna:* 39% *C. elegans:* 19%	*D. magna:* 26–58% *C. elegans:* 34%	CCND1 (*Homo sapiens*) was well conserved across all vertebrates at Level 1, with the similarity value of Level 2 being significantly higher than the one of Level 1 across all taxa including *D. magna*
	CDKN1A/ p21	*Homo sapiens*	Fish: 19–26% Amphibians: 25% Birds: 30% Mammals: 71–77%	Fish: 47–56% Amphibians: 63% Birds: 62% Mammals: 92–94%	*D. magna:* 13% *C. elegans:* 12%	*D. magna:* 39% *C. elegans:* 32%	CDKN1A (*Homo sapiens*) showed a low degree of conservation in fish, amphibians and birds as well as in *D. magna* for Level 1. However, Level 2 similarity values were consistently higher than those at Level 1 across all vertebrate and invertebrate taxa.
	PCNA	*Xenopus laevis*	Fish: 90–91% Birds: 90.73% Mammals: 93%	Fish: 90–92% Birds: 91% Mammals: 93%	*D. magna:* 76% *C. elegans:* 50%	*D. magna:* 76% *C. elegans:* 50%	PCNA (*Xenopus laevis*) was well conserved, with high similarity values for Level 1 and Level 2

(*continued on next page*)

Table 5 (*continued*)

Biological pathway	Targets assessed	Reference species	Vertebrate conservation (Level 1: full sequence)	Vertebrate conservation (Level 2: functional domain(s))	Invertebrate conservation (Level 1: full sequence)	Invertebrate conservation (Level 2: functional domain)	Key conclusions
Neuronal/cardiac signalling	AChE	*Danio rerio*	Fish: 73–90% Amphibians: 61% Birds: 51% Mammals: 57–58%	Fish: 73–100% Amphibians: 61–84% Birds: 54–61% Mammals: 57–91%	*D. magna:* 35% *C. elegans:* 32%	*D. magna:* 38% *C. elegans:* 35%	across all vertebrates and invertebrates. AChE (*Danio rerio*), was highly conserved across vertebrates at both levels, while the degree of conservation was low in invertebrates at both levels.

characterisation.

Overall MoA conclusion

The integration of the curated bioactivity dataset, pathway enrichment analysis, SeqAPASS analysis and apical endpoint correlation collectively identified eleven mechanistically distinct MoA pathway categories for TCS (Table 4). These four independent lines of evidence converged consistently: the pathway categories identified from endpoint-level bioactivity data were independently confirmed by gene-set enrichment across three species; the molecular targets at the lower end of the effect concentration spectrum were shown to be structurally and functionally conserved across ecotoxicologically relevant taxa; and the MoA pathways mapped coherently to downstream apical outcomes, with bioactivity thresholds being consistently lower than apical effect concentrations.

The *HMGCS2* mRNA response in primary human hepatocytes is considered here as an early molecular indicator of disrupted PPAR-mediated lipid metabolism, rather than an isolated transcriptional change. *HMGCS2* is a known PPARα target gene within the PPAR signalling and lipid metabolism pathway, which was itself independently identified in the curated bioactivity dataset and supported by gene-set enrichment. The target shows sequence conservation across all assessed vertebrate taxa and in *Daphnia magna* at both Level 1 and Level 2.

The *HMGCS2* mRNA upregulation at 0.007 μg/L was the lowest effect concentration in the curated bioactivity dataset and was carried forward as the candidate ePoD for Step 8. Given the cross-species conservation of the target, this value is expected to be protective for taxa without direct empirical data, including fish and aquatic invertebrates.

Tier 2: Application of *ab initio* approach

Step 7: targeted testing and biokinetic refinement

Step 7 includes two components: targeted NAMs testing to strengthen the MoA hypothesis (Step 7a), and biokinetic refinement for QIVIVE or PBK model parameterisation (Step 7b). For the purpose of this case study, neither component required the generation of new experimental data.

For Step 7a, targeted NAMs testing was not considered necessary because TCS is a data-rich compound with an extensive mechanistic and bioactivity dataset available in the public domain. The curated dataset provided sufficient coverage across a broad range of biological endpoints to support pathway identification and hypothesis formulation without additional testing. The analysis of this dataset revealed consistent perturbation of key pathways including nuclear receptor signalling, lipid and steroid metabolism, thyroid axis activity, and oxidative stress, which collectively contributed to the formulation of the MoA hypothesis and the ePoD derivation.

For Step 7b, biokinetic refinement was not required because measured intrinsic clearance data for TCS were already available from cryopreserved rainbow trout hepatocytes (Black et al., 2021), as described in Step 5. These data provided the empirical basis for the QIVIVE factor derivation without the need for additional *in vitro* clearance measurements. The QIVIVE factor derived in Step 5 was applied directly to the bioactivity dataset to convert nominal *in vitro* effect concentrations to external aqueous concentration equivalents for the integration with the *in vivo* ecotoxicity records. PBK modelling was not developed for this case study, as the one-compartment QIVIVE approach was considered sufficient for this case study.

Step 8: hazard assessment and identification of ePoD

The ePoD was derived by two parallel routes to provide both a conservative lower-bound estimate and a species-distribution-based estimate. Both routes were based on the integrated TCS hazard dataset, which combined empirical *in vivo* ecotoxicity data for algae and aquatic invertebrates (including *Daphnia magna*), read-across-derived ecotoxicity values for vertebrate species from diclosan, and QIVIVE-corrected *in vitro* NAM-derived effect concentrations expressed as external aqueous concentration equivalents (Step 5).

For the lowest-PoD approach, effect concentrations were compiled using the integrated dataset across all taxonomic groups and the most sensitive endpoint identified. The lowest value was *HMGCS2* mRNA upregulation in primary human hepatocytes at 0.007 μg/L, derived from the QIVIVE-corrected NAM data. Given the sequence conservation of *HMGCS2* across vertebrates and in *D. magna* (see Step 6), this value was taken forward as the conservative ePoD. An assessment factor of 1 was applied on the basis of two considerations. First, the *HMGCS2* mRNA expression effect concentration was the lowest value across the integrated dataset, making it inherently conservative as an ePoD. Second, the conservation of *HMGCS2* across vertebrates and in *D. magna* at both Level 1 and Level 2 supports the cross-species applicability of the ePoD without further adjustment. No additional quantitative correction beyond the applied QIVIVE step was introduced at this stage. The resulting PNEC—NGRA-lowest was set at 0.007 μg/L.

The HMGCS2-based ePoD should therefore be interpreted as a conservative lower-bound estimate within the integrated weight-of-evidence framework, rather than as a directly apical protective threshold in the conventional ERA sense. This value is used as a protective decision anchor for comparison with exposure. In fact, it is below the lowest effect concentrations identified for all other biological pathway categories (Table 4) and is 1.6- to 413-folds lower; it is also below the lowest available apical ecotoxicity effect concentration of 0.1 μg/L for algae and aquatic invertebrates. The selected ePoD therefore lies at the lower end of the available data across molecular, cellular and organism-level responses.

The application of an assessment factor of 1 does not imply absence of uncertainty around this molecular response. Rather, it avoids adding an additional default factor to an endpoint that was already selected as the lower bound of the complete integrated dataset and that is supported by pathway-level evidence, cross-species conservation and consistency

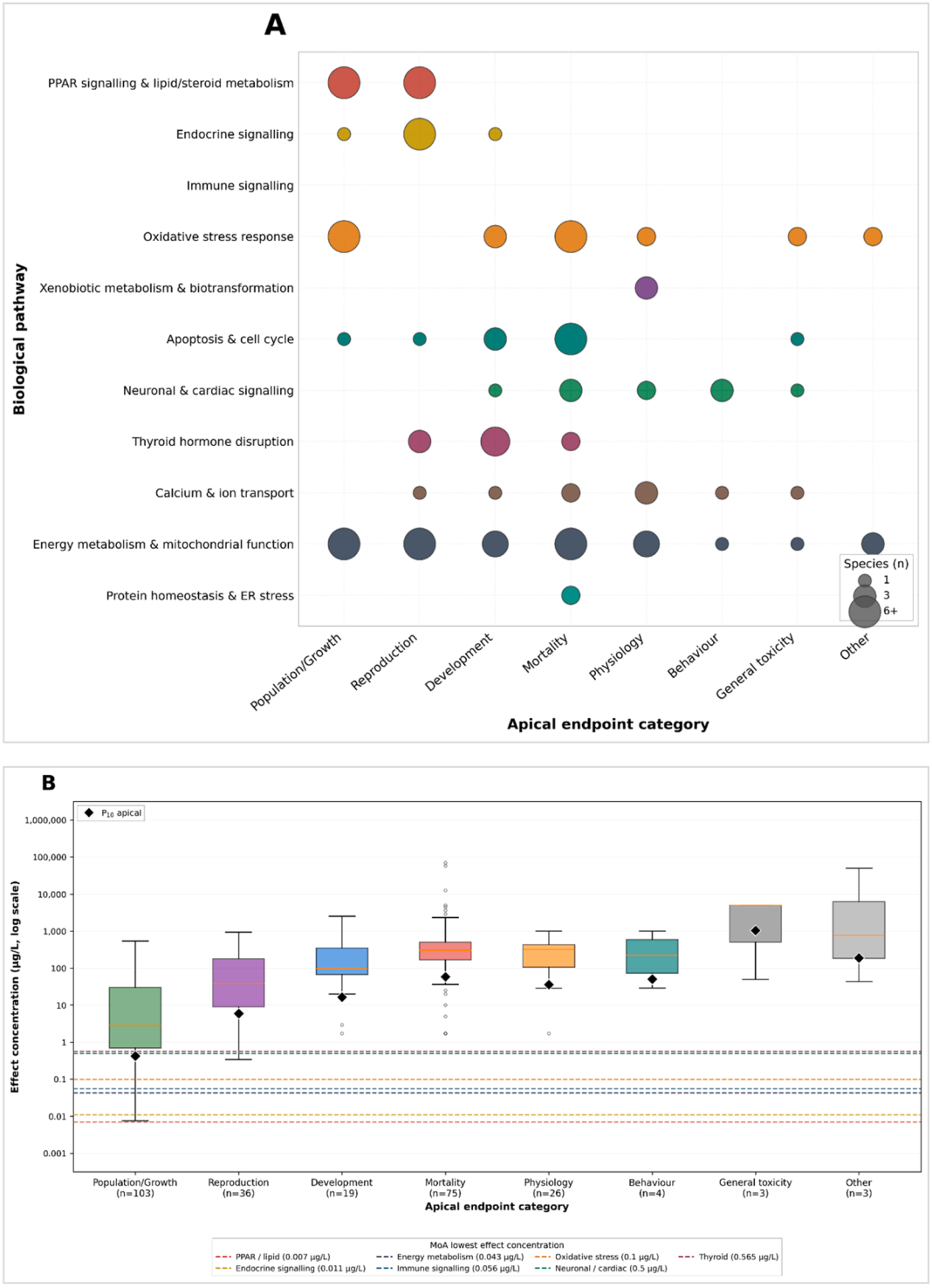

Fig. 6. Correlation between MoA bioactivity and apical endpoint effect concentrations for TCS.
(A) Dot matrix showing the mapping of biological pathway categories (rows) to apical endpoint categories (columns) based on mechanistic relevance. Each dot indicates a confirmed association between a biological pathway and an apical endpoint category within the ecotoxicological dataset (excluding NAM-derived data); the dot size is proportional to the number of species in which the association was observed. The absence of a dot indicates no mechanistic linkage. Pathways are ordered by their lowest bioactivity effect concentration (ascending). Dot colour corresponds to the biological pathway. The 269 apical records across 50 species yielded 618 pathway–apical associations. **(B)** Box plot showing the distribution of apical endpoint effect concentrations (µg/L, log scale), grouped by apical endpoint category and ordered identically to Panel A. Sample sizes are indicated below each category. Black diamonds denote the 10th percentile (P10) of apical effect concentrations for each category. Dashed horizontal lines indicate the lowest MoA bioactivity effect concentration for each pathway category, colour-coded to match the pathway palette in Panel A and identified in the legend below the plot with their corresponding concentration values (µg/L). The position of all MoA thresholds below the P10 of apical effect concentrations across endpoint categories confirms that molecular-level effects are consistently detectable at concentrations lower than organism-level adverse outcomes. Figure generated using Python (matplotlib v3.10).

with apical effect concentrations.

For the SSD-based approach, a species sensitivity distribution was developed using the integrated dataset described above, including algae, terrestrial invertebrates, aquatic invertebrates, fish, amphibians, birds and mammals. *In vitro* NAMs data and *in vivo* aquatic ecotoxicity data were combined to broaden the biological coverage of the SSD, so that the hazard threshold is a statistical estimate across species rather than a single sentinel endpoint. Mammalian and avian NAM data were included on the general NGRA assumption that low-concentration bioactivity contributes to cross-species hazard characterisation, when the underlying molecular targets are conserved across taxa. Conservation was demonstrated via SeqAPASS for the targets driving the lower end of the effect concentration spectrum (Step 6), the data points that anchor the conservative ePoD. In case *in vitro* NAM data were used, AC_{50}, LEC and NOAEC values from the curated bioactivity dataset were included after QIVIVE correction (Step 5). The SSD was developed using the US EPA SSD Toolbox v.1.1 (Etterson, 2020). The Weibull distribution was selected as the best-fitting model based on the corrected Akaike Information Criterion (AICc: 441.4, Akaike weight: 0.71), yielding an HC_{05} of 0.20 μg/L (log HC_{05}: −0.70) based on geometric mean effect concentrations across 44 species. The model-averaged HC_{05} across all distributions evaluated was 0.194 μg/L (Fig. 7). An assessment factor of 10 was applied to the HC_{05} to reflect two sources of residual uncertainty: the heterogeneous nature of the integrated dataset, which combined *in vivo* ecotoxicity endpoints with QIVIVE-corrected *in vitro* effect concentrations; and the absence of normalisation to a common effect metric across the integrated dataset. The resulting PNEC—NGRA-SSD was 0.020 μg/L.

Step 9: exposure and risk assessment

The refined PEC was derived using the Mintel market data on TCS-containing cosmetics as the use-input, from which annual $PEC_{surface\ water}$ values were derived for the period 2015 to 2025 (refer to **Supplementary Data 3**). $PEC_{surface\ water}$ declined progressively over this period, from 0.017 μg/L in 2015 to 0.0021 μg/L in 2025, reflecting a reduction in TCS occurrence in cosmetic products following regulatory restrictions. The refined central PEC range of 0.0021–0.0079 μg/L covers 2018 onwards, when TCS use had substantially declined from peak levels (see Table 6).

The distribution of NAMs-derived effect concentrations relative to these annual PEC values and the two NAM-derived PNECs is illustrated in Fig. 8, which shows that the majority of bioactivity data points across all taxonomic groups are at concentrations well above the refined PEC range, and that the PNECs are at the lower end of the mammalian and aquatic vertebrate bioactivity distributions.

The RCR was calculated by dividing the annual refined PEC by each of the two NAM-derived PNECs, and the results are summarised in Table 7. An RCR below 1 indicates that the PEC is below the PNEC and a low-concern conclusion is supported; an RCR above 1 indicates that the

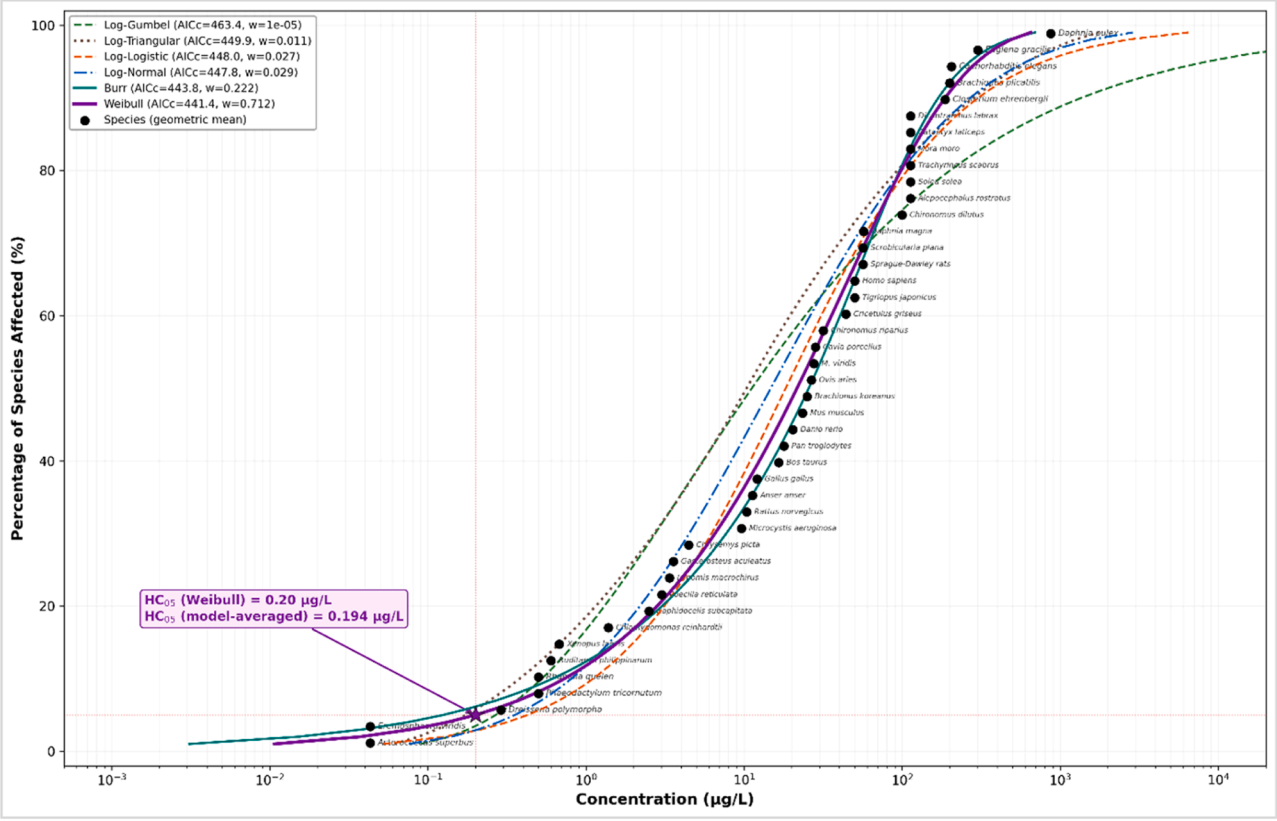

Fig. 7. SSD for TCS based on NAMs data, including bioactivity (AC50, BMD, LEC, NOEC) and omics-derived effect concentrations expressed as external aqueous equivalents following QIVIVE correction.

Data points represent geometric mean effect concentrations per species (n: 44 species, black circles), plotted against the cumulative percentage of species affected (see **Supplementary Data 9**). Six distribution models were fitted via maximum likelihood estimation using the US EPA SSD Toolbox v.1.1 (Etterson, 2020): Weibull (solid purple), Burr (solid teal), log-normal (blue dash-dot), log-logistic (orange dashed), log-triangular (brown dotted), and log-Gumbel (green dashed). The Weibull distribution was selected as the best-fitting model based on the corrected Akaike Information Criterion (AICc = 441.4, Akaike weight w = 0.71), yielding an HC_{05} of 0.20 μg/L (purple star), representing the hazardous concentration protective of 95% of species. The model-averaged HC_{05} across all six distributions evaluated was 0.194 μg/L. Horizontal and vertical red dotted lines mark the 5th-percentile intersection corresponding to the Weibull HC_{05} of 0.20 μg/L on the concentration axis. Distribution fitting and model selection were carried out in the US EPA SSD Toolbox v.1.1. Python (scipy v.1.17.1, matplotlib v.3.10.8) was used to compute the species geometric means, position the data points using the Hazen formula [(i − 0.5)/n], and draw the figure from the Toolbox's AICc results and fitted curves.

Table 6
Refined Predicted Effect Concentrations in surface water ($PEC_{surface\ water}$).

	2015	2016	2017	2018	2019	2020	2021	2022	2023	2024	2025
$PEC_{surface\ water}$ (µg/L)	0.017	0.015	0.011	0.0079	0.0053	0.0048	0.0044	0.0038	0.0027	0.0022	0.0021

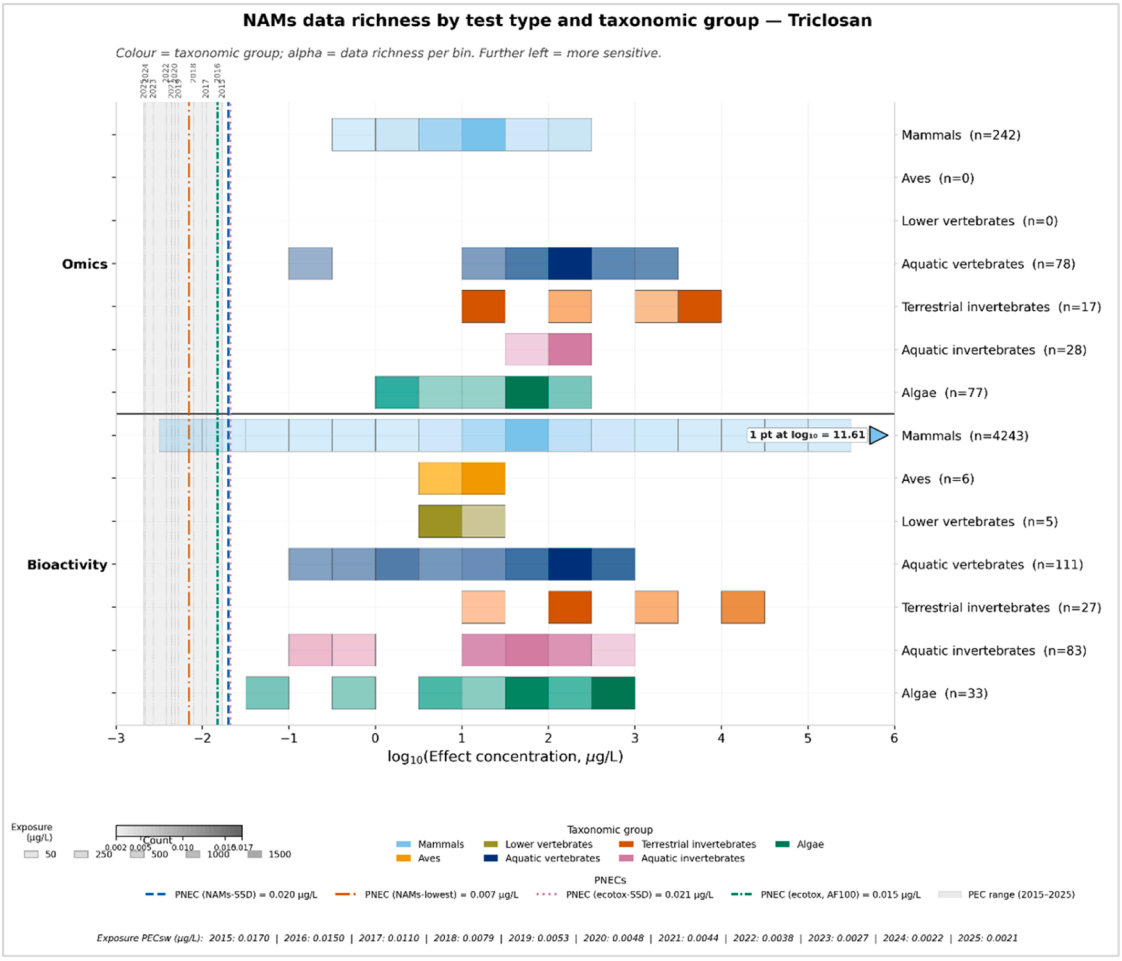

Fig. 8. Horizontal histogram showing the distribution of NAMs-derived effect concentrations for TCS across taxonomic groups and test types.
The upper panel presents omics data (transcriptomics, metabolomics and proteomics) and the lower panel presents bioactivity data (AC_{50}, BMD, LEC and NOEC), separated by a horizontal divider. Each row represents a taxonomic group; bar colour indicates the taxonomic group: bluish green (algae), reddish purple (aquatic invertebrates), blue (aquatic vertebrates), orange (aves), sky blue (mammals), olive (lower vertebrates), and vermillion (terrestrial invertebrates, C. elegans). Bar opacity (alpha) is proportional to the number of data points per concentration bin (log_{10}-scaled, 0.5-unit bins), with darker shading indicating greater data richness. The grey shaded band indicates the range of refined market data-driven $PEC_{surface\ water}$ values from 2015 (0.017 µg/L) to 2025 (0.0021 µg/L), with individual years marked by vertical grey lines. Four PNEC values are overlaid as vertical lines: PNEC (NAMs-SSD): 0.020 µg/L (blue dashed), PNEC (NAMs-lowest): 0.007 µg/L (orange dash-dot), PNEC (ecotox-SSD): 0.021 µg/L (purple dotted), and PNEC (ecotox, AF100): 0.015 µg/L (green dash-dot-dot). Sample sizes per taxonomic group and test type are shown in parentheses on the right y-axis. Effect concentrations for mammalian and avian *in vitro* data are expressed as external aqueous equivalents following QIVIVE correction. Figure generated using Python (matplotlib v.3.10).

PEC exceeds the PNEC and a potential risk cannot be excluded. Using the SSD-based PNEC—NGRA of 0.020 µg/L, RCR values remained below 1 for all years assessed, decreasing from 0.83 in 2015 to 0.10 in 2025.

Using the lowest-PoD PNEC—NGRA of 0.007 µg/L, RCR values exceeded 1 in 2015–2018 (2.43 for 2015, 2.14 for 2016, 1.57 for 2017, and 1.14 for 2018), reflecting higher TCS market penetration during that period. From 2019 onwards, RCR values were below 1, decreasing from 0.71 in 2019 to 0.29 in 2025.

The two NGRA-derived PNECs were interpreted as complementary decision anchors rather than as competing alternative thresholds. The PNEC—NGRA-SSD provides a distribution-based estimate derived from the integrated dataset across species and endpoint types, whereas the PNEC—NGRA-lowest represents a conservative lower-bound estimate based on the most sensitive mechanistically supported bioactivity endpoint. Together, the two values define a decision range for the ENV NGRA assessment.

The PNEC—NGRA-lowest was used as the protective decision anchor for comparison against the refined PEC. The PNEC—NGRA-lowest (0.007 µg/L) and PNEC—NGRA-SSD (0.024 µg/L) agree within a factor of approximately 3, supporting confidence in the assessment.

A low-concern conclusion is strongest when the refined PEC is below both values. If the refined PEC falls between the two PNECs, this would not automatically indicate unacceptable risk, but would identify a zone wwhere targeted refinement is warranted, for example through improved exposure characterisation, biokinetic refinement of the QIVIVE step, or generation of additional NAM data to test whether

Table 7
Risk characterisation ratios (RCRs).

Year	Exposure $PEC_{surface\ water}$ (µg/L)	PNEC (NGRA-SSD) (µg/L)	RCR	PNEC (NGRA-lowest) (µg/L)	RCR
2015	0.017	0.020	0.83	0.007	2.43
2016	0.015		0.74		2.14
2017	0.011		0.55		1.57
2018	0.008		0.39		1.14
2019	0.005		0.27		0.71
2020	0.005		0.24		0.71
2021	0.004		0.22		0.57
2022	0.004		0.19		0.57
2023	0.003		0.13		0.43
2024	0.002		0.11		0.29
2025	0.002		0.10		0.29

HMGCS2 upregulation represents an adverse or adaptive response.

The refined $PEC_{surface\ water}$ values were below both NAM-derived PNECs from 2019 onwards. This represents the exit point for the ENV NGRA workflow, with the RCR confirmed below 1 from 2019 onwards using both derivation approaches, based on the refined use-based exposure estimate.

Step 10: assessment of the level of confidence and evaluation of potential uncertainties

The overall level of confidence in the ENV NGRA risk conclusion was assessed as high for the refined post-2019 exposure scenario, while recognising medium confidence in some individual quantitative assumptions, particularly the exact numerical value of the QIVIVE-derived lowest ePoD. This judgement is supported by three main considerations. First, the TCS bioactivity and ecotoxicity dataset is unusually large and covers many species across multiple taxonomic groups, reducing the need for default uncertainty factors and providing robust species sensitivity coverage. Second, both NAM-derived PNECs (0.007 µg/L and 0.020 µg/L) remain above the refined use-based PEC range of 0.0021 to 0.0053 µg/L applicable from 2019 onwards, yielding RCR values below 1 under both derivation approaches for this period (see **Step 9** and Table 6). Third, SeqAPASS analysis showed that *HMGCS2*, the most sensitive biological target driving the lowest ePoD, is conserved across the key ecotoxicological test species, supporting the cross-species biological relevance of this endpoint. Additional considerations that reinforce this assessment include: (1) HMGCS2 is part of the lipid metabolism and PPARα signalling pathway, which was identified as enriched and conserved across the species analysed, providing pathway-level biological plausibility for the endpoint; (2) The PNEC—NGRA-lowest and PNEC—NGRA-SSD agree within a factor of approximately 3, and provide internal corroboration between two independently derived routes; and (3) both NAM-derived PNECs are within the same order of magnitude as the externally derived REACH PNEC for TCS, and this provides additional external benchmarking.

With respect to exposure, pre-2019 $PEC_{surface\ water}$ values ranging from 0.0079 to 0.017 µg/L exceeded the PNEC—NGRA-lowest of 0.007 µg/L, consistent with the period of higher TCS market penetration prior to regulatory restrictions. The high-confidence risk conclusion is therefore specific to the refined post-2019 exposure scenario. With respect to the hazard assessment, the QIVIVE model relies on a one-compartment model and may introduce up to an order of magnitude of uncertainty in the biokinetic conversion. This uncertainty affects the interpretation of the two derivation routes differently. For the lowest-ePoD route, the effect is approximately linear because the HMGCS2-based ePoD is directly derived from a QIVIVE-corrected *in vitro* concentration. A plausible downward shift in the external concentration equivalent would therefore materially affect the RCRs derived from the lowest-ePoD route, whereas an upward shift would increase the margin. This sensitivity is the reason why the HMGCS2-based value is interpreted as a conservative lower-bound decision anchor rather than as a stand-alone regulatory threshold. For the SSD route, the influence of QIVIVE uncertainty is less direct because the SSD integrates *Multiple species*, test systems and endpoint types, including non-QIVIVE-corrected *in vivo* ecotoxicity values. A formal quantitative perturbation analysis of the QIVIVE factor was not performed in this case study. However, confidence in the overall risk conclusion is supported by the concordance between the SSD-based NGRA PNEC, the ecotoxicity-based comparator PNEC and independently derived regulatory thresholds.

A further source of uncertainty relates to the heterogeneity of effect metrics across the dataset. AC_{50}, LEC and NOAEC values were compared directly after QIVIVE correction, without normalisation to a common dose descriptor. Although AC_{50} is widely accepted as a valid *in vitro* bioactivity concentration for NAMs-based hazard assessment (Paul Friedman et al., 2020), AC_{50} and threshold-based descriptors, such as NOAEC and LEC, correspond to different points on the concentration-response curve, and their direct comparison introduces residual uncertainty in the relative sensitivity ranking of endpoints and species.

Taken together, these residual uncertainties qualify the confidence in individual numerical thresholds, particularly the exact value of the QIVIVE-derived lowest ePoD. They do not, however, undermine the overall conclusion for the refined post-2019 exposure scenario, because the risk characterisation is supported by multiple convergent lines of evidence, including the SSD-based NGRA PNEC, the conservative lowest-ePoD anchor, the ecotoxicity-based comparator and external regulatory benchmarks. The framework exits at Step 10 with the conclusion that, under the refined use-based exposure scenario, PEC is below both NAM-derived PNECs from 2019 onwards, supporting a low concern conclusion for this period.

Discussion

This study demonstrates that the 10-step NGRA framework originally developed for cosmetic ingredient human health safety assessment (Alexander-White et al., 2022; Najjar et al., 2024) is applicable to environmental safety, while maintaining its tiered assessment structure. The transfer does not require a fundamental change to the framework architecture; rather, it involves domain-specific substitution of several key inputs, methods and decision criteria.

Human systemic exposure is replaced by environmental exposure expressed as PEC, and human pharmacokinetic modelling is replaced by QIVIVE as the primary biokinetic correction. TTC concepts are substituted with ecoTTC values calibrated to aquatic species sensitivity, while mammalian receptor-based bioactivity data are complemented by aquatic ecotoxicity endpoints, cross-species conservation analysis and ecotoxicological MoA analysis. Throughout the workflow, mechanistic pathway reasoning provides the overarching interpretive framework.

As a result, the exposure-led, hypothesis-driven, tiered logic of the original framework is retained. The present case study supports the operational applicability of this transfer for a cosmetic ingredient, while also highlighting methodological aspects that require further development before routine application across broader chemical classes and exposure scenarios. These aspects are discussed in the following sections.

Four core principles guided the adaptation of the HH NGRA framework to the environmental domain in this study.

First, the assessment must be anchored to a realistic exposure. Environmental NGRA begins from realistic release and exposure scenarios rather than from hazard data considered in isolation, so that hazard characterisation is calibrated to the environmental concentrations.

Second, mechanistic evidence must be used to explain ecological risk rather than merely to detect biological activity, with NAM outputs being interpreted in a biologically meaningful context, which considers pathways, cross-species relevance and ecological plausibility.

Third, NAM-derived information must be translated into environmentally relevant thresholds, as the value of NAMs in environmental NGRA depends on converting mechanistic signals into effect concentrations that can be quantitatively compared with PECs.

Fourth, the framework must remain protective and transparent, applying conservative conclusions where appropriate, explicitly addressing uncertainty, and benchmarking outputs against conventional ERA whenever possible.

Together, these principles adapt the general logic of the ICCR NGRA principles to the environmental domain. The foundation principles described by Dent and collaborators remain highly relevant to environmental NGRA (Dent et al., 2018). However, the overall protection goal requires reformulation: rather than human safety, environmental NGRA targets ecological receptors, with the protection of populations, communities and ecosystems as the underlying objective.

Applying TCS across all ten steps exercised the framework end to end and confirmed that it can handle a chemically complex, data-rich substance without early exit. At Tier 0, the conservative lower tier screening PEC of 0.74 μg/L exceeded the endocrine based ecoTTC and the interim read across PNECs and, therefore, did not support an early low concern conclusion. Although comparison with the conventional REACH PNEC of 0.843 μg/L would give an RCR below 1, that PNEC relies on vertebrate ecotoxicity data that were excluded from the present NGRA workflow by design. Progression to subsequent tiers was therefore required to derive analogue- and NAM-based thresholds on a non-animal data basis, and to benchmark their protectiveness against conventional ERA thresholds.

At Tier 2, NGRA-based effect thresholds were derived via two complementary approaches: a lowest-ePoD approach and an SSD based on an integrated dataset. For the SSD-based approach, the integrated dataset combined *in vivo* ecotoxicity values for algae and aquatic invertebrates, read-across-derived ecotoxicity (diclosan as the read-across substance), and QIVIVE-corrected *in vitro* NAM-derived effect concentrations expressed as external aqueous equivalents. The integrated curve covered 44 species across seven taxonomic groups (algae, aquatic invertebrates, terrestrial invertebrates, fish, amphibians, birds and mammals), and yielded a Weibull-derived HC_{05} of 0.20 μg/L. Combining *in vivo* aquatic toxicity data with *in vitro* toxicity information has precedent in PNEC derivation; Guo and colleagues applied AF- and SSD-based approaches to benzophenone-type UV filters using both data streams (Guo et al., 2020). The same bridging logic was applied to the lowest-ePoD approach, consistent with a recent assessment by Rivetti and colleagues, where the lowest PoD across an integrated *in vitro* and *in vivo* dataset served as the anchor for the risk decision (Rivetti et al., 2025).

The integrated SSD broadens species coverage, but the limitation is the dose-descriptor heterogeneity. AC50, LEC and NOAEC values were compared directly after QIVIVE correction without normalisation to a common effect metric. AC50 is widely accepted as a valid *in vitro* PoD for NAMs-based hazard assessment, but AC50, NOAEC and LEC represent different positions on the concentration-response curve; combining them within one SSD introduces lower tail uncertainty that is difficult to quantify without metric harmonisation. The AF of 10 applied to the resulting HC_{05} was justified specifically as a partial mitigation for descriptor heterogeneity and the lack of normalisation, rather than as a generic safety margin. The lowest-ePoD route avoids the curve-fitting step and the descriptor-heterogeneity problem that comes with it.

The parallel lowest-PoD PNEC was reported using an AF of 1, which was based on *HMGCS2* mRNA induction, a transcriptional marker of PPARα-driven lipid metabolism perturbation, as the most sensitive endpoint, with SeqAPASS confirming conservation across species. PPARα-driven ketogenesis and lipid mobilisation, when sustained, have been linked in fish to reduced energy reserves for vitellogenesis and embryonic development (Ho et al., 2016; Tocher, 2003). This provides a plausible mechanism linking the transcriptional response to the reproduction and development endpoints captured in the apical dataset. Carrying both routes forward enabled the SSD-derived PNEC and the lowest-ePoD PNEC to be obtained independently from the same dataset and compared directly. Future development should prioritise dose-descriptor harmonisation in the SSD route. Schaupp and colleagues showed that the choice of *in vitro* descriptor affects the level of correlation between ToxCast PoDs and *in vivo* ECOTOX endpoints, with the lowest concentration of bioactivity across all assays correlating more strongly than 5th-centile activity concentration at cut-off (ACC5) values (Schaupp et al., 2023). This supports the use of a response-consistent metric rather than AC50 or mixed descriptors before SSD development.

A further direction for methodological development concerns the SSD development itself. A Bayesian SSD would be a useful comparator for the parametric construction used here (Fox et al., 2021) for two practical reasons. First, it returns the HC_{05} as a probability distribution with a credible interval rather than as a single point estimate, making uncertainty around the protective threshold explicit. Second, it allows differential weighting of individual data points, so that QIVIVE-corrected *in vitro* values and *in vivo* apical values can contribute according to their relative ecological relevance and dose-descriptor stringency rather than as equivalent points. Both features fit the type of integrated dataset used here, which combines data of different origin (*in vitro* and *in vivo*) and different effect metrics (AC50, NOAEC and LEC). A Bayesian comparison would test whether the point estimate from the parametric construction masks uncertainty that matters to regulatory interpretation. An additional caveat is that the US EPA SSD Toolbox v1.1 used here was developed for conventional apical whole-organism data under standardised conditions (Posthuma et al., 2019; Wheeler et al., 2002). Applying it to an integrated *in vitro/in vivo* dataset is feasible with careful curation, but it lies outside its original use case; a software tool designed for integrated NAM and apical data would therefore be a logical next development.

Benchmarking the NGRA-derived PNECs against existing regulatory thresholds provides an important line of confidence in the case study. Published thresholds for TCS range from 0.005 μg/L (Danish EPA saltwater EQS (Miljøministeriet, 2010)) to 0.843 μg/L (REACH PNEC derived using SSD with AF 1 (ECHA CHEM, 2026)). This range reflects differences in the underlying ecotoxicity datasets, derivation methods and assessment factors across regulatory bodies (see **Table S4 in the Supplementary Data 2**). This variation across regulatory thresholds for the same substance is part of the reason a structured environmental NGRA approach with explicit derivation assumptions adds value, even for a well-studied compound. Within this regulatory range, the PNEC—NGRA-SSD of 0.020 μg/L derived in the present case study is essentially identical to Swiss Centre for Applied Ecotoxicology / Oekotoxzentrum annual average-EQS (AA-EQS) of 0.02 μg/L (derived from a NOEC with AF 10) (Casado-Martinez, 2021) and the SCHEER maximum allowable concentration - quality standard for freshwater (MAC-QSfw) of 0.019 μg/L (derived from an ErC50 with AF 100) (SCHEER, 2023), and the conventional ecotox-SSD PNEC of 0.021 μg/L derived from the same study without *in vitro* inclusion. This convergence between the NGRA SSD and several independently derived regulatory thresholds indicates that the integrated SSD development yields a value consistent with established regulatory practice when *in vitro* data are added. The PNEC—NGRA-lowest of 0.007 μg/L falls between the Danish EPA saltwater EQS (0.005 μg/L) and the Danish EPA freshwater EQS (0.01 μg/L), consistent with a single-target value anchored on a conserved molecular endpoint. Both NGRA-derived PNECs are approximately 1.5 to 2 orders of magnitude lower than the REACH PNEC, consistent with patterns observed in human-health NGRA case studies where NAM-based PoDs tend to be conservative relative to conventional NOAELs (Ebmeyer et al., 2024; Najjar et al., 2024; Paul Friedman et al., 2020). Agreement observed for a single, data-rich substance does not constitute validation across chemical classes. However, convergence between the NGRA SSD-based PNEC and several existing regulatory thresholds, together with the more conservative lowest-PoD PNEC, supports the position that the framework is not systematically under-protective.

Species diversity is the structural difference that distinguishes

environmental NGRA from its human-health counterpart. Human-health NGRA can build on biological coverage centred on *Homo sapiens*, whereas environmental NGRA has to cover algae, aquatic and terrestrial invertebrates, fish, amphibians, birds and mammals, with each group being represented by multiple species in regulatory practice. Dedicated environmental NAMs remain comparatively scarce. While methods such as *Rainbow trout* gill-Waterloo 1 (RTgill-W1) (OECD TG 249) (Tanneberger et al., 2013), zebrafish embryo toxicity assays, *Daphnia magna* behavioural endpoints and algal transcriptomics are increasingly available, much of the high-throughput bioactivity evidence underpinning NAMs-based hazard assessment is still derived from human-health NAMs. In the present case study, this constraint was addressed in two ways. The bioactivity dataset was assembled to cover a wide range of biological targets across taxa, capturing diversity at the pathway and target level rather than relying on species-level testing alone. Cross-species conservation analysis with SeqAPASS (Doering et al., 2018; LaLone et al., 2018, 2016) provided an independent line of evidence that the targets driving the candidate ePoD are conserved, with HMGCS2 in particular meeting the conservation threshold for Level 1 (primary amino acid sequence) and level 2 (functional domain conservation) across the assessed vertebrates and in D. magna. Bioactivity diversity and cross-species conservation analysis partially addresses the species coverage problem, but a complete solution requires the development and broader adoption of dedicated environmental NAMs, particularly for algae, invertebrates and birds. Wider availability of such methods would reduce the reliance on bridging from human-health NAMs and place more of the evidence base on direct, species-relevant data.

QIVIVE is another area where environmental application lags that in the human health domain. The one-compartment PBK model used here for prediction of fish BCF (Krause and Goss, 2020) - which has been parameterised with *in vitro* hepatic intrinsic clearance from rainbow trout hepatocytes (Black et al., 2021) - is a workable approximation for a freshwater fish exposure scenario and provides a QIVIVE factor of 0.0039. Equivalent compartmental models for algae, invertebrates and birds are less developed, and aquatic kinetic models remain less mature and less validated than the PBK models used routinely in HH NGRA (Grech et al., 2019; Wetmore et al., 2012). Where target-organ-specific risk characterisation is required in future applications, species-specific PBK models could provide tissue-level internal concentration estimates for direct comparison with the internal effect concentrations from the *in vitro* assays used to derive the PoD. Maturation of multi-compartment PBK models across the major receptor groups would broaden the species coverage that QIVIVE can support and would reduce the residual uncertainty introduced by the one-compartment approximation.

The framework as demonstrated applies to neutral organic chemicals in the freshwater compartment. Other substance classes and compartments will require targeted methodological adaptation before they can be assessed with the same level of confidence. Highly volatile substances need additional treatment of volatilisation losses at the exposure stage (OECD, 2019). Substances of unknown or variable composition, complex reaction products or biological materials (UVCBs) and mixtures require careful read across to handle compositional variability. Metals require speciation and bioavailability modelling. Ionisable organics need pH-dependent partitioning incorporated into the QIVIVE step (Escher et al., 2020). Sediment, terrestrial and marine compartments each have distinct exposure dynamics and protection goals that would require compartment-specific adaptation. The underlying tiered logic of the framework remains relevant across these contexts, but the methods at each step need purposeful development before they can be applied routinely. Confidence in environmental NGRA as a practical assessment approach will grow through demonstrated performance across substance classes, MoA categories and exposure scenarios. The most important next test is the application of the framework to a data-poor substance with low predicted exposure, since the framework's tiered, exit-at-low-concern logic is designed precisely for that scenario. A substance with low predicted exposure may exit at Tier 0 (Alexander-White et al., 2022; Berggren et al., 2017) on the basis of structural screening and ecoTTC comparison alone. Substances with lower tier PECs above conservative screening thresholds, such as TCS, progress through the subsequent tiers, where the available data richness determines how informatively each step can be exercised. Standardised curation and normalisation approaches across NAMs datasets are an active area of methodological development (Daniel et al., 2022) and will be a necessary input as the case study evidence base grows. The convergence between human-health and environmental NGRA observed in this case study, in which the same 10-step structure transferred with limited methodological adjustment, points towards a broader integration opportunity. Human-health and environmental risk assessment have traditionally run on separate tracks, but the exposure pathway they share (substances applied to skin reaching aquatic systems) and the increasing recognition that AOPs anchor mechanistic reasoning across both human and ecological receptors (LaLone et al., 2018) make a stronger case for integration than has generally been acknowledged. NGRA, built around mechanistic reasoning and hypothesis-driven structure, is well placed to bridge that gap, and this case study is one step in that direction. This supports the broader view that NAM- based assessment is most informative when applied within a structured, tiered and problem driven framework, rather than as a collection of isolated methods.

Conclusion

This case study demonstrates how the 10-step NGRA framework can be applied to environmental safety assessment. The four ENV NGRA core principles articulated in the Discussion guided the transfer of the framework from human-health assessment to environmental safety assessment adaptation. When applied to triclosan (TCS), the framework progressed through all ten steps without the generation of new vertebrate data and produced two complementary NGRA-derived PNECs, both of which are consistent with independently derived regulatory thresholds for the same substance.

The PNEC—NGRA-SSD of 0.02 μg/L is essentially identical to the Swiss Centre for Applied Ecotoxicology / Oekotoxzentrum AA-EQS of 0.02 μg/L (derived from a NOEC with AF 10) (Casado-Martinez, 2021) and the SCHEER MAC-QSfw of 0.019 μg/L (derived from an ErC50 with AF 100) (SCHEER, 2023), despite the different derivation routes underlying these values. The more conservative PNEC—NGRA-lowest of 0.007 μg/L falls within the protective range defined by the Danish EPA freshwater (0.01 μg/L) and saltwater (0.005 μg/L) EQS values. This convergence supports the conclusion that the integrated SSD development, despite combining *in vivo* and QIVIVE-corrected *in vitro* endpoints, yields a value that is consistent with established regulatory practice on a data-rich substance. The value of the framework lies in offering a structured, mechanistic and transparent route to environmental risk decisions that can be exercised end to end without new animal testing.

The risk conclusion should be interpreted in the context of the refined post-2019 exposure scenario. For this period, the refined PEC remained below both complementary NGRA-derived PNECs, supporting a low-concern conclusion. Confidence in this conclusion is high at the overall weight-of-evidence level, while the exact numerical value of individual decision anchors, particularly the QIVIVE-derived lowest ePoD, remains associated with greater uncertainty.

Several methodological priorities emerge from the present work. Dose-descriptor harmonisation through ACC- or EC10-equivalent conversions and benchmarking of the parametric SSD against a Bayesian SSD are practical next steps for the SSD route. Maturation of PBK modelling for environmentally relevant species is required to broaden the applicability of the QIVIVE bridge across taxa. Continued development of dedicated environmental NAMs, together with cross-species conservation analysis using SeqAPASS (including Level 3 assessments where Level 1 conservation is intermediate), will strengthen confidence

in extrapolation from human-health NAMs to non-mammalian species. The most informative next test of the framework would be its application to a data-poor substance with low predicted exposure. Such a case would exercise the framework's exit-at-low-concern logic at Tier 0, complementing the present case where the full ten-step progression was intentionally exercised.

Substance classes outside neutral organic chemicals in freshwater systems will require targeted methodological adaptations. Taken together, the present work demonstrates that the 10-step NGRA framework is operationally transferable from human-health to environmental safety, that the resulting NAMs-based PNECs are consistent with established regulatory thresholds for the same substance, and that the methodological gaps identified are tractable through continued case studies and targeted development. The work is offered as a step towards an integrated next-generation safety paradigm in which mechanistic reasoning supports decision-making across both human-health and environmental protection goals. This supports the broader view that NAM-based assessment is most informative when applied within a structured, tiered and problem-driven framework rather than as a collection of isolated methods.

Declaration of generative AI and AI-assisted technologies in the manuscript preparation process

During the preparation of this manuscript, the authors used Microsoft Copilot and OpenAI ChatGPT to support language editing, improve readability and assist with grammatical and stylistic refinement. These tools were not used to generate the scientific concept, study design, assessment strategy, data analysis, calculations, interpretation of results, figures, tables or conclusions. All AI-assisted suggestions were critically reviewed, edited and approved by the authors, who take full responsibility for the content of the published article.

CRediT authorship contribution statement

Harald Streicher: Writing – review & editing, Writing – original draft, Supervision, Methodology, Formal analysis, Data curation, Conceptualization. **Sanghamitra Mishra:** Writing – review & editing, Writing – original draft, Visualization, Methodology, Data curation, Conceptualization. **Zakaria Naddi:** Writing – review & editing, Methodology, Investigation, Formal analysis, Data curation. **Rita Fernandes:** Writing – review & editing, Investigation, Formal analysis, Data curation. **Monica Autiero:** Writing – review & editing, Methodology, Data curation, Conceptualization. **Sophia Krause:** Methodology, Investigation, Formal analysis. **Avneet Kaur Suri:** Methodology, Investigation, Data curation. **Celine De Roy:** Methodology, Investigation, Data curation. **Andreas Schepky:** Writing – review & editing, Methodology, Conceptualization. **Abdulkarim Najjar:** Writing – review & editing, Methodology, Conceptualization.

Declaration of competing interest

The authors declare that they have no known competing financial interests or personal relationships that could have appeared to influence the work reported in this paper.

Acknowledgements

The authors gratefully acknowledge Dr. Thomas Petry for his overall supervision and constructive input throughout the development of this case study on behalf of Toxminds. We also thank Dr. Shruta Dadarkar (Beiersdorf AG) for her valuable support during the initiation phase of the collaboration and for facilitating the early alignment between Beiersdorf and Toxminds. We further thank Dr. Steffen Erler (Beiersdorf AG) for his constructive input and valuable scientific discussions throughout the process. Their contributions were instrumental in enabling this work.

Supplementary materials

Supplementary material associated with this article can be found, in the online version, at doi:10.1016/j.namjnl.2026.100106.

Data availability

Data will be made available on request.

References

Abramson, H.N., 2011. The lipogenesis pathway as a cancer target. J. Med. Chem. 54, 5615–5638. https://doi.org/10.1021/jm2005805.

Alexander-White, C., Bury, D., Cronin, M., Dent, M., Hack, E., Hewitt, N.J., Kenna, G., Naciff, J., Ouedraogo, G., Schepky, A., Mahony, C., Europe, C., 2022. A 10-step framework for use of read-across (RAX) in next generation risk assessment (NGRA) for cosmetics safety assessment. Regul. Toxicol. Pharmacol. 129, 105094. https://doi.org/10.1016/j.yrtph.2021.105094.

Alpizar F., Backhaus T., Decker N., Eilks I., Escobar-Pemberthy N., Fantke P., Geiser K., Ivanova M., Jolliet O., Kim H.S. 2019. UN Environment global chemicals outlook II - from legacies to innovative solutions: implementing the 2030 agenda for sustainable development.

Ankley, G.T., Bennett, R.S., Erickson, R.J., Hoff, D.J., Hornung, M.W., Johnson, R.D., Mount, D.R., Nichols, J.W., Russom, C.L., Schmieder, P.K., Serrrano, J.A., Tietge, J. E., Villeneuve, D.L., 2010. Adverse outcome pathways: a conceptual framework to support ecotoxicology research and risk assessment. Environ. Toxicol. Chem. 29, 730–741. https://doi.org/10.1002/etc.34.

Bedoux, G., Roig, B., Thomas, O., Dupont, V., Le Bot, B., 2012. Occurrence and toxicity of antimicrobial triclosan and by-products in the environment. Environ. Sci. Pollut. Res. Int. 19, 1044–1065. https://doi.org/10.1007/s11356-011-0632-z.

Benfenati, E., Manganaro, A., Gini, G.C., 2013. VEGA-QSAR: AI inside a platform for predictive toxicology. *In* (ed). In: Proceedings of the 2nd Workshop on Popularize Artificial Intelligence, PAI 2013, Held in Conjunction with AI*IA. In PAI@ AI* IA. Turin, Italy, pp. 21–28.

Berggren, E., White, A., Ouedraogo, G., Paini, A., Richarz, A.N., Bois, F.Y., Exner, T., Leite, S., Grunsven, L.A.V., Worth, A., Mahony, C., 2017. *Ab initio* chemical safety assessment: a workflow based on exposure considerations and non-animal methods. Comput. Toxicol. 4, 31–44. https://doi.org/10.1016/j.comtox.2017.10.001.

Bester, K., 2003. Triclosan in a sewage treatment process-balances and monitoring data. Water Res. 37, 3891–3896. https://doi.org/10.1016/S0043-1354(03)00335-X.

Black, S.R., Nichols, J.W., Fay, K.A., Matten, S.R., Lynn, S.G., 2021. Evaluation and comparison of *in vitro* intrinsic clearance rates measured using cryopreserved hepatocytes from humans, rats, and rainbow trout. Toxicology 457, 152819. https://doi.org/10.1016/j.tox.2021.152819.

Briggs, K., Barber, C., Cases, M., Marc, P., Steger-Hartmann, T., 2015. Value of shared preclinical safety studies–The eTOX database. Toxicol. Rep. 2, 210–221. https://doi.org/10.1016/j.toxrep.2014.12.004.

Bury, D., Alexander-White, C., Clewell 3rd, H.J., Cronin, M., Desprez, B., Detroyer, A., Efremenko, A., Firman, J., Hack, E., Hewitt, N.J., Kenna, G., Klaric, M., Lester, C., Mahony, C., Ouedraogo, G., Paini, A., Schepky, A., Cosmetics, E., 2021. New framework for a non-animal approach adequately assures the safety of cosmetic ingredients–A case study on caffeine. Regul. Toxicol. Pharmacol. 123, 104931. https://doi.org/10.1016/j.yrtph.2021.104931.

Capdevielle, M., Van Egmond, R., Whelan, M., Versteeg, D., Hofmann-Kamensky, M., Inauen, J., Cunningham, V., Woltering, D., 2008. Consideration of exposure and species sensitivity of triclosan in the freshwater environment. Integr. Environ. Assess. Manag. 4, 15–23. https://doi.org/10.1897/IEAM_2007-022.1.

Casado-Martinez, C., 2021. SQC (EQSsed)–Proposal by the Ecotox Centre for: Triclosan. Lausanne (CH): Swiss Centre for Applied Ecotoxicology, p. 32 pp. https://www.oekotoxzentrum.ch/media/195638/0_triclosan_june2022.pdf.

Connors, K.A., Beasley, A., Barron, M.G., Belanger, S.E., Bonnell, M., Brill, J.L., de Zwart, D., Kienzler, A., Krailler, J., Otter, R., Phillips, J.L., Embry, M.R., 2019. Creation of a curated aquatic toxicology database: EnviroTox. Environ. Toxicol. Chem. 38, 1062–1073. https://doi.org/10.1002/etc.4382.

Crombie, T.A., Pamminger, T., Andersen, E.C., Glaberman, S., 2026. High-throughput toxicity screening with *C. elegans*: current platforms, key advantages, and future directions. Environ. Sci. Technol. https://doi.org/10.1021/acs.est.5c12562.

Daniel, A.B., Choksi, N., Abedini, J., Bell, S., Ceger, P., Cook, B., Karmaus, A.L., Rooney, J., To, K.T., Allen, D., Kleinstreuer, N., 2022. Data curation to support toxicity assessments using the integrated chemical environment. Front. Toxicol. 4, 987848. https://doi.org/10.3389/ftox.2022.987848.

Danish (Q)SAR Database, 2026. Danish (Q)SAR Database, On Nordic Council of Minister, European Chemicals Agency (ECHA). Ministry of Environment of Denmark and DTU National Food Institute. http://qsar.food.dtu.dk/ (accessed in).

Danish EPA, 2016. Survey of Triclosan in Cosmetic Products. Survey of Chemical Substances in Consumer Products No. 152. Danish Environmental Protection Agency, Copenhagen. https://www2.mst.dk/Udgiv/publications/2016/12/978-87-93529-47-2.pdf.

Davis, A.P., Wiegers, T.C., Johnson, R.J., Sciaky, D., Wiegers, J., Mattingly, C.J., 2023. Comparative toxicogenomics database (CTD): update 2023. Nucleic Acids Res. 51, D1257–D1262. https://doi.org/10.1093/nar/gkac833.

De Roy, C., Mishra, S., Petry, T., Tencalla, F., Autiero, M., 2022. SOC-III-09 comparison of key players involved in endocrine-related effects across different vertebrate species. Toxicol. Lett. 368, S45–S46. https://doi.org/10.1016/j.toxlet.2022.07.143.

de Wolf, W., Siebel-Sauer, A., Lecloux, A., Koch, V., Holt, M., Feijtel, T., Comber, M., Boeije, G., 2005. Mode of action and aquatic exposure thresholds of no concern. Environ. Toxicol. Chem. 24, 479–485. https://doi.org/10.1897/04-133R.1.

Dent, M., Amaral, R.T., Da Silva, P.A., Ansell, J., Boisleve, F., Hatao, M., Hirose, A., Kasai, Y., Kern, P., Kreiling, R., Milstein, S., Montemayor, B., Oliveira, J., Richarz, A., Taalman, R., Vaillancourt, E., Verma, R., Posada, N.V.O.R.C., Weiss, C., Kojima, H., 2018. Principles underpinning the use of new methodologies in the risk assessment of cosmetic ingredients. Comput. Toxicol. 7, 20–26. https://doi.org/10.1016/j.comtox.2018.06.001.

Di Nicola, M.R., Cattaneo, I., Nathanail, A.V., Carnesecchi, E., Astuto, M.C., Steinbach, M., Williams, A.J., Charles, S., Gestin, O., Lopes, C., 2023. The use of new approach methodologies for the environmental risk assessment of food and feed chemicals. Curr. Opin. Environ. Sci. Health 31, 100416. https://doi.org/10.1016/j.coesh.2022.100416.

Doering, J.A., Lee, S., Kristiansen, K., Evenseth, L., Barron, M.G., Sylte, I., LaLone, C.A., 2018. *In silico* site-directed mutagenesis informs species-specific predictions of chemical susceptibility derived from the Sequence Alignment to Predict Across Species Susceptibility (SeqAPASS) tool. Toxicol. Sci. 166, 131–145. https://doi.org/10.1093/toxsci/kfy186.

Du, G., Yu, M., Wang, L., Hu, W., Song, L., Lu, C., Wang, X., 2018. Transcriptome and DNA methylome dynamics during triclosan-induced cardiomyocyte differentiation toxicity. Stem Cells Int. 2018, 8608327. https://doi.org/10.1155/2018/8608327.

Dulio, V., Koschorreck, J., Van Bavel, B., Van den Brink, P., Hollender, J., Munthe, J., Schlabach, M., Aalizadeh, R., Agerstrand, M., Ahrens, L., 2020. The NORMAN association and the European partnership for chemicals risk assessment (PARC): let's cooperate. Environ. Sci. Eur. 32, 100. https://doi.org/10.1186/s12302-020-00375-w.

EAWAG. 2026. EAWAG-BBD pathway prediction system. https://eawag-bbd.ethz.ch/predict/(accessed in).

Ebmeyer, J., Najjar, A., Lange, D., Boettcher, M., Voss, S., Brandmair, K., Meinhardt, J., Kuehnl, J., Hewitt, N.J., Krueger, C.T., Schepky, A., 2024. Next generation risk assessment: an *ab initio* case study to assess the systemic safety of the cosmetic ingredient, benzyl salicylate, after dermal exposure. Front. Pharmacol. 15, 1345992. https://doi.org/10.3389/fphar.2024.1345992.

EC. 2012. Commission implementing decision of 14 November 2012 establishing a common format for the submission of the information pursuant to Directive 2010/63/EU of the European Parliament and of the Council on the protection of animals used for scientific purposes (notified under document C(2012) 8064) (2012/707/EU). Report No. L 320/33, https://eur-lex.europa.eu/legal-content/EN/TXT/HTML/?uri=CELEX%3A32012D0707&utm.

EC. 2020. Commission staff working document. Accompanying the document - report from the commission to the European parliament and the council: 2019 report on the statistics on the use of animals for scientific purposes in the Member States of the European Union in 2015-2017. Report No. SWD(2020) 10 final, European Commission, https://eur-lex.europa.eu/legal-content/EN/TXT/HTML/?uri=CELEX%3A52020SC0010&.

ECHA, 2008. Guidance on Information Requirements and Chemical Safety Assessment Chapter R.10: Characterisation of Dose [Concentration]–Response for Environment. European Chemicals Agency, 2008. https://echa.europa.eu/documents/10162/13632/information_requirements_r10_en.pdf/bb902be7-a503-4ab7-9036-d866b8ddce69.

ECHA CHEM. 2026. REACH registration of triclosan (CAS number: 3380-34-5; EC number: 222-182-2). https://chem.echa.europa.eu/100.020.167/overview?searchText=triclosan (accessed in).

ECHA PACT. 2025. Public activities coordination tool - triclosan. https://echa.europa.eu/fr/pact (accessed in).

ECHA/EFSA, 2018. Guidance for the identification of endocrine disruptors in the context of Regulations (EU) No 528/2012 and (EC) No 1107/2009. EFSA J. 16, e05311. https://doi.org/10.2903/j.efsa.2018.5311.

EnviroTox. 2026. EnviroTox database search (version 2.0.0 - updated 28 September 2021) - triclosan. https://envirotoxdatabase.org/(accessed in).

Escher, B.I., Abagyan, R., Embry, M., Kluver, N., Redman, A.D., Zarfl, C., Parkerton, T.F., 2020. Recommendations for improving methods and models for aquatic hazard assessment of ionizable organic chemicals. Environ. Toxicol. Chem. 39, 269–286. https://doi.org/10.1002/etc.4602.

Etterson M. 2020. Technical manual: SSD toolbox version 1.0.

EU, 2009. Regulation (EC) No 1223/2009 of the European parliament and of the council of 30 November 2009 on cosmetic products. L 342/59. Off. J. Eur. Union. https://eur-lex.europa.eu/legal-content/EN/TXT/PDF/?uri=CELEX:32009R1223&from=EN.

EU. 2012. Consolidated text: regulation (EU) No 528/2012 of the European Parliament and of the Council of 22 May 2012 concerning the making available on the market and use of biocidal products. https://eur-lex.europa.eu/legal-content/EN/TXT/?uri=CELEX:02012R0528-20240611.

EU. 2024. Commission regulation (EU) 2024/996 of 3 April 2024 amending Regulation (EC) No 1223/2009 of the European Parliament and of the Council as regards the use of Vitamin A, Alpha-Arbutin and Arbutin and certain substances with potential endocrine disrupting properties in cosmetic products. Report No. OJ.L.4.4.2024, https://eur-lex.europa.eu/legal-content/EN/TXT/PDF/?uri=OJ%3AL_202400996&utm.

EU REACH, 2006. Regulation (EC) No 1907/2006 of the European Parliament and of the Council of 18 December 2006 concerning the Registration, Evaluation, Authorisation and Restriction of Chemicals (REACH), establishing a European Chemicals Agency, amending Directive 1999/45/EC and repealing Council Regulation (EEC) No 793/93 and Commission Regulation (EC) No 1488/94 as well as Council Directive 76/769/EEC and Commission Directives 91/155/EEC, 93/67/EEC, 93/105/EC and 2000/21/EC (Text with EEA relevance). OJ L 396. Off. J. Eur. Union. https://eur-lex.europa.eu/legal-content/EN/ALL/?uri=CELEX%3A32006R1907.

Forte, M., Mita, L., Cobellis, L., Merafina, V., Specchio, R., Rossi, S., Mita, D.G., Mosca, L., Castaldi, M.A., De Falco, M., Laforgia, V., Crispi, S., 2016. Triclosan and bisphenol a affect decidualization of human endometrial stromal cells. Mol. Cell. Endocrinol. 422, 74–83. https://doi.org/10.1016/j.mce.2015.11.017.

Fox, D.R., van Dam, R.A., Fisher, R., Batley, G.E., Tillmanns, A.R., Thorley, J., Schwarz, C.J., Spry, D.J., McTavish, K., 2021. Recent developments in species sensitivity distribution modeling. Environ. Toxicol. Chem. 40, 293–308. https://doi.org/10.1002/etc.4925.

Fu, J., Gong, Z., Kelly, B.C., 2019. Metabolomic profiling of zebrafish (*Danio rerio*) embryos exposed to the antibacterial agent triclosan. Environ. Toxicol. Chem. 38, 240–249. https://doi.org/10.1002/etc.4292.

Gene Ontology Consortium, Aleksander, S.A., Balhoff, J., Carbon, S., Cherry, J.M., Drabkin, H.J., Ebert, D., Feuermann, M., Gaudet, P., Harris, N.L., Hill, D.P., Lee, R., Mi, H., Moxon, S., Mungall, C.J., Muruganugan, A., Mushayahama, T., Sternberg, P.W., Thomas, P.D., Van Auken, K., Ramsey, J., Siegele, D.A., Chisholm, R.L., Fey, P., Aspromonte, M.C., Nugnes, M.V., Quaglia, F., Tosatto, S., Giglio, M., Nadendla, S., Antonazzo, G., Attrill, H., Dos Santos, G., Marygold, S., Strelets, V., Tabone, C.J., Thurmond, J., Zhou, P., Ahmed, S.H., Asanitthong, P., Luna Buitrago, D., Erdol, M.N., Gage, M.C., Ali Kadhum, M., Li, K.Y.C., Long, M., Michalak, A., Pesala, A., Pritazahra, A., Saverimuttu, S.C.C., et al., 2023. The gene ontology knowledgebase in 2023. Genetics 224. https://doi.org/10.1093/genetics/iyad031.

Gomes, M.F., de Carvalho Soares de Paula, V., Rocha Martins, L.R., Esquivel Garcia, J.R., Yamamoto, F.Y., Martins de Freitas, A., 2021. Sublethal effects of triclosan and triclocarban at environmental concentrations in silver catfish (*Rhamdia quelen*) embryos. Chemosphere 263, 127985. https://doi.org/10.1016/j.chemosphere.2020.127985.

Grech, A., Tebby, C., Brochot, C., Bois, F.Y., Bado-Nilles, A., Dorne, J.L., Quignot, N., Beaudouin, R., 2019. Generic physiologically-based toxicokinetic modelling for fish: integration of environmental factors and species variability. Sci. Total Environ. 651, 516–531. https://doi.org/10.1016/j.scitotenv.2018.09.163.

Gross, M., Daginnus, K., Deviller, G., de Wolf, W., Dungey, S., Galli, C., Gourmelon, A., Jacobs, M., Matthiessen, P., Micheletti, C., Nestmann, E., Pavan, M., Paya-Perez, A., Ratte, H.T., Safford, B., Sokull-Kluttgen, B., Stock, F., Stolzenberg, H.C., Wheeler, J., Willuhn, M., Worth, A., Comenges, J.M., Crane, M., 2010. Thresholds of toxicological concern for endocrine active substances in the aquatic environment. Integr. Environ. Assess. Manag. 6, 2–11. https://doi.org/10.1897/IEAM_2008-092.1.

Guo, Q., Wei, D., Zhao, H., Du, Y., 2020. Predicted no-effect concentrations determination and ecological risk assessment for benzophenone-type UV filters in aquatic environment. Environ. Pollut. 256, 113460. https://doi.org/10.1016/j.envpol.2019.113460.

Gutsell, S., Hodges, G., Marshall, S., Roberts, J., 2015. Ecotoxicological thresholds-practical application to an industrial inventory. Environ. Toxicol. Chem. 34, 935–942. https://doi.org/10.1002/etc.2875.

Haggard, D.E., Noyes, P.D., Waters, K.M., Tanguay, R.L., 2016. Phenotypically anchored transcriptome profiling of developmental exposure to the antimicrobial agent, triclosan, reveals hepatotoxicity in embryonic zebrafish. Toxicol. Appl. Pharmacol. 308, 32–45. https://doi.org/10.1016/j.taap.2016.08.013.

Halden, R.U., Paull, D.H., 2005. Co-occurrence of triclocarban and triclosan in U.S. water resources. Environ. Sci. Technol. 39, 1420–1426. https://doi.org/10.1021/es049071e.

Harrill, J.A., Everett, L.J., Haggard, D.E., Sheffield, T., Bundy, J.L., Willis, C.M., Thomas, R.S., Shah, I., Judson, R.S., 2021. High-throughput transcriptomics platform for screening environmental chemicals. Toxicol. Sci. 181, 68–89. https://doi.org/10.1093/toxsci/kfab009.

Hewitt, N.J., Troutman, J., Przibilla, J., Schepky, A., Ouedraogo, G., Mahony, C., Kenna, G., Varcin, M., Dent, M.P., Europe, C., 2022. Use of *in vitro* metabolism and biokinetics assays to refine predicted *in vivo* and *in vitro* internal exposure to the cosmetic ingredient, phenoxyethanol, for use in risk assessment. Regul. Toxicol. Pharmacol. 131, 105132. https://doi.org/10.1016/j.yrtph.2022.105132.

Ho, J.C.H., Hsiao, C.D., Kawakami, K., Tse, W.K.F., 2016. Triclosan (TCS) exposure impairs lipid metabolism in zebrafish embryos. Aquat. Toxicol. 173, 29–35. https://doi.org/10.1016/j.aquatox.2016.01.001.

Houck, K.A., Simha, A., Bone, A., Doering, J.A., Vliet, S.M.F., LaLone, C., Medvedev, A., Makarov, S., 2021. Evaluation of a multiplexed, multispecies nuclear receptor assay for chemical hazard assessment. Toxicol. *In Vitro* 72, 105016. https://doi.org/10.1016/j.tiv.2020.105016.

Hunt, P.R., 2017. The *C. elegans* model in toxicity testing. J. Appl. Toxicol. 37, 50–59. https://doi.org/10.1002/jat.3357.

Kanehisa, M., Goto, S., 2000. KEGG: kyoto encyclopedia of genes and genomes. Nucleic Acids Res. 28, 27–30. https://doi.org/10.1093/nar/28.1.27.

Kenda, M., Karas Kuzelicki, N., Iida, M., Kojima, H., Sollner Dolenc, M., 2020. Triclocarban, triclosan, bromochlorophene, chlorophene, and climbazole effects on nuclear receptors: an in silico and *in vitro* study. Environ. Health Perspect. 128, 107005. https://doi.org/10.1289/ehp6596.

Kim, J., Oh, H., Ryu, B., Kim, U., Lee, J.M., Jung, C.R., Kim, C.Y., Park, J.H., 2018. Triclosan affects axon formation in the neural development stages of zebrafish embryos (*Danio rerio*). Environ. Pollut. 236, 304–312. https://doi.org/10.1016/j.envpol.2017.12.110.

Kim, J.Y., Yi, B.R., Go, R.E., Hwang, K.A., Nam, K.H., Choi, K.C., 2014. Methoxychlor and triclosan stimulates ovarian cancer growth by regulating cell cycle- and apoptosis-related genes via an estrogen receptor-dependent pathway. Environ. Toxicol. Pharmacol. 37, 1264–1274. https://doi.org/10.1016/j.etap.2014.04.013.

Klimisch, H.J., Andreae, M., Tillmann, U., 1997. A systematic approach for evaluating the quality of experimental toxicological and ecotoxicological data. Regul. Toxicol. Pharmacol. 25, 1–5. https://doi.org/10.1006/rtph.1996.1076.

Kloas, W., Urbatzka, R., Opitz, R., Wurtz, S., Behrends, T., Hermelink, B., Hofmann, F., Jagnytsch, O., Kroupova, H., Lorenz, C., Neumann, N., Pietsch, C., Trubiroha, A., Van Ballegooy, C., Wiedemann, C., Lutz, I., 2009. Endocrine disruption in aquatic vertebrates. Ann. NY Acad. Sci. 1163, 187–200. https://doi.org/10.1111/j.1749-6632.2009.04453.x.

Krause, S., Goss, K.U., 2020. Comparison of a simple and a complex model for BCF prediction using *in vitro* biotransformation data. Chemosphere 256, 127048. https://doi.org/10.1016/j.chemosphere.2020.127048.

LaLone, C.A., Villeneuve, D.L., Doering, J.A., Blackwell, B.R., Transue, T.R., Simmons, C. W., Swintek, J., Degitz, S.J., Williams, A.J., Ankley, G.T., 2018. Evidence for cross species extrapolation of mammalian-based high-throughput screening assay results. Environ. Sci. Technol. 52, 13960–13971. https://doi.org/10.1021/acs.est.8b04587.

LaLone, C.A., Villeneuve, D.L., Lyons, D., Helgen, H.W., Robinson, S.L., Swintek, J.A., Saari, T.W., Ankley, G.T., 2016. Editor's highlight: sequence Alignment to Predict Across Species Susceptibility (SeqAPASS): a web-based tool for addressing the challenges of cross-species extrapolation of chemical toxicity. Toxicol. Sci. 153, 228–245. https://doi.org/10.1093/toxsci/kfw119.

Langan, L.M., Paparella, M., Burden, N., Constantine, L., Margiotta-Casaluci, L., Miller, T. H., Moe, S.J., Owen, S.F., Schaffert, A., Sikanen, T., 2024. Big question to developing solutions: a decade of progress in the development of aquatic new approach methodologies from 2012 to 2022. Environ. Toxicol. Chem. 43, 559–574. https://doi.org/10.1002/etc.5578.

Leung, M.C.K., Williams, P.L., Benedetto, A., Au, C., Helmcke, K.J., Aschner, M., Meyer, J.N., 2008. *Caenorhabditis elegans*: an emerging model in biomedical and environmental toxicology. Toxicol. Sci. 106, 5–28. https://doi.org/10.1093/toxsci/kfn121.

Lu, S., Archer, M.C., 2005. Fatty acid synthase is a potential molecular target for the chemoprevention of breast cancer. Carcinogenesis 26, 153–157. https://doi.org/10.1093/carcin/bgh278.

Mackay, D., McCarty, L.S., Arnot, J.A., 2014. Relationships between exposure and dose in aquatic toxicity tests for organic chemicals. Environ. Toxicol. Chem. 33, 2038–2046. https://doi.org/10.1002/etc.2649.

Margiotta-Casaluci, L., Owen, S.F., Winter, M.J., 2024. Cross-species extrapolation of biological data to guide the environmental safety assessment of pharmaceuticals-the state of the art and future priorities. Environ. Toxicol. Chem. 43, 513–525. https://doi.org/10.1002/etc.5634.

Marshall, N.B., Lukomska, E., Long, C.M., Kashon, M.L., Sharpnack, D.D., Nayak, A.P., Anderson, K.L., Jean Meade, B., Anderson, S.E., 2015. Triclosan induces thymic stromal lymphopoietin in skin promoting Th2 allergic responses. Toxicol. Sci. 147, 127–139. https://doi.org/10.1093/toxsci/kfv113.

Matozzo, V., Formenti, A., Donadello, G., Marin, M.G., 2012. A multi-biomarker approach to assess effects of triclosan in the clam *Ruditapes philippinarum*. Mar. Environ. Res. 74, 40–46. https://doi.org/10.1016/j.marenvres.2011.12.002.

Milacic, M., Beavers, D., Conley, P., Gong, C., Gillespie, M., Griss, J., Haw, R., Jassal, B., Matthews, L., May, B., Petryszak, R., Ragueneau, E., Rothfels, K., Sevilla, C., Shamovsky, V., Stephan, R., Tiwari, K., Varusai, T., Weiser, J., Wright, A., Wu, G., Stein, L., Hermjakob, H., D'Eustachio, P., 2024. The Reactome pathway knowledgebase 2024. Nucleic Acids Res. 52, D672–D678. https://doi.org/10.1093/nar/gkad1025.

Miljøministeriet. 2010. Fastsættelse af kvalitetskriterier for vandmiljøet: triclosan (CAS number: 3380-34-5). https://mst.dk/media/xzmlalgf/triclosan-3380-34-5.pdf.

Mintel, 2026. Mintel Global New Products Database (GNPD). London: Mintel Group Ltd. Proprietary database. https://www.mintel.com/products/gnpd/ (accessed in May 2026).

Mitchell, C.A., Burden, N., Bonnell, M., Hecker, M., Hutchinson, T.H., Jagla, M., LaLone, C.A., Lagadic, L., Lynn, S.G., Shore, B., Song, Y., Vliet, S.M., Wheeler, J.R., Embry, M.R., 2023. New approach methodologies for the endocrine activity toolbox: environmental assessment for fish and amphibians. Environ. Toxicol. Chem. 42, 757–777. https://doi.org/10.1002/etc.5584.

Moss, T., Howes, D., Williams, F.M., 2000. Percutaneous penetration and dermal metabolism of triclosan (2,4, 4′-trichloro-2′-hydroxydiphenyl ether). Food Chem. Toxicol. 38, 361–370. https://doi.org/10.1016/s0278-6915(99)00164-7.

Najjar, A., Kuhnl, J., Lange, D., Genies, C., Jacques, C., Fabian, E., Zifle, A., Hewitt, N.J., Schepky, A., 2024. Next-generation risk assessment read-across case study: application of a 10-step framework to derive a safe concentration of daidzein in a body lotion. Front. Pharmacol. 15, 1421601. https://doi.org/10.3389/fphar.2024.1421601.

NICNAS, 2009. Priority Existing Chemical Assessment Report Number 30: Triclosan. National Industrial Chemicals Notification and Assessment Scheme. https://www.industrialchemicals.gov.au/sites/default/files/PEC30-Triclosan.pdf.

NORMAN Association. 2026. NORMAN EMPODAT database - chemical occurrence data. https://www.norman-network.com/nds/empodat/chemicalSearch.php (accessed in May 2026).

Nyffeler, J., Willis, C., Lougee, R., Richard, A., Paul-Friedman, K., Harrill, J.A., 2020. Bioactivity screening of environmental chemicals using imaging-based high-throughput phenotypic profiling. Toxicol. Appl. Pharmacol. 389, 114876. https://doi.org/10.1016/j.taap.2019.114876.

OECD. 2019. Guidance document on aquatic toxicity testing of difficult substances and mixtures. Series on testing and assessment No. 23 (second edition). Report No. ENV/JM/MONO(2000)6/REV1, https://www.oecd.org/en/publications/guidance-document-on-aquatic-toxicity-testing-of-difficult-substances-and-mixtures_0ed2f88e-en.html.

OECD. 2024. The OECD QSAR toolbox (v.4.7) for grouping chemicals into categories. https://qsartoolbox.org/download/(accessed in May 2026).

Oekotoxzentrum, 2021. SQC (EQSsed)–Proposal By the Ecotox Centre for: Triclosan. Oekotoxzentrum Centre Ecotox. https://www.oekotoxzentrum.ch/media/195638/0_triclosan_june2022.pdf.

Olker, J.H., Elonen, C.M., Pilli, A., Anderson, A., Kinziger, B., Erickson, S., Skopinski, M., Pomplun, A., LaLone, C.A., Russom, C.L., Hoff, D., 2022. The ECOTOXicology Knowledgebase: a curated database of ecologically relevant toxicity tests to support environmental research and risk assessment. Environ. Toxicol. Chem. 41, 1520–1539. https://doi.org/10.1002/etc.5324.

Ouedraogo, G., Alexander-White, C., Bury, D., Clewell 3rd, H.J., Cronin, M., Cull, T., Dent, M., Desprez, B., Detroyer, A., Ellison, C., Giammanco, S., Hack, E., Hewitt, N. J., Kenna, G., Klaric, M., Kreiling, R., Lester, C., Mahony, C., Mombelli, E., Naciff, J., O'Brien, J., Schepky, A., Tozer, S., van der Burg, B., van Vugt-Lussenburg, B., Stuard, S., Cosmetics, E., 2022. Read-across and new approach methodologies applied in a 10-step framework for cosmetics safety assessment–A case study with parabens. Regul. Toxicol. Pharmacol. 132, 105161. https://doi.org/10.1016/j.yrtph.2022.105161.

Parenti, C.C., Ghilardi, A., Della Torre, C., Mandelli, M., Magni, S., Del Giacco, L., Binelli, A., 2019. Environmental concentrations of triclosan activate cellular defence mechanism and generate cytotoxicity on zebrafish (*Danio rerio*) embryos. Sci. Total Environ. 650, 1752–1758. https://doi.org/10.1016/j.scitotenv.2018.09.283.

Paul Friedman, K., Gagne, M., Loo, L.H., Karamertzanis, P., Netzeva, T., Sobanski, T., Franzosa, J.A., Richard, A.M., Lougee, R.R., Gissi, A., Lee, J.J., Angrish, M., Dorne, J. L., Foster, S., Raffaele, K., Bahadori, T., Gwinn, M.R., Lambert, J., Whelan, M., Rasenberg, M., Barton-Maclaren, T., Thomas, R.S., 2020. Utility of *in vitro* bioactivity as a lower bound estimate of *in vivo* adverse effect levels and in risk-based prioritization. Toxicol. Sci. 173, 202–225. https://doi.org/10.1093/toxsci/kfz201.

Posthuma, L., van Gils, J., Zijp, M.C., van de Meent, D., de Zwart, D., 2019. Species sensitivity distributions for use in environmental protection, assessment, and management of aquatic ecosystems for 12 386 chemicals. Environ. Toxicol. Chem. 38, 905–917. https://doi.org/10.1002/etc.4373.

ProtoPRED. 2025. ProtoPRED. ProtoQSAR SL. https://protopred.protoqsar.com/ProtoTOX_info (accessed in May 2026).

Queiros, L., Pereira, J.L., Goncalves, F.J.M., Pacheco, M., Aschner, M., Pereira, P., 2019. *Caenorhabditis elegans* as a tool for environmental risk assessment: emerging and promising applications for a "nobelized worm". Crit. Rev. Toxicol. 49, 411–429. https://doi.org/10.1080/10408444.2019.1626801.

Richard, A.M., Huang, R., Waidyanatha, S., Shinn, P., Collins, B.J., Thillainadarajah, I., Grulke, C.M., Williams, A.J., Lougee, R.R., Judson, R.S., Houck, K.A., Shobair, M., Yang, C., Rathman, J.F., Yasgar, A., Fitzpatrick, S.C., Simeonov, A., Thomas, R.S., Crofton, K.M., Paules, R.S., Bucher, J.R., Austin, C.P., Kavlock, R.J., Tice, R.R., 2021. The Tox21 10K compound ibrary: collaborative chemistry advancing toxicology. Chem. Res. Toxicol. 34, 189–216. https://doi.org/10.1021/acs.chemrestox.0c00264.

Rivetti, C., Campos, B., 2023. Establishing a NexGen, mechanism-based environmental risk assessment paradigm shift: are we ready yet? Integr. Environ. Assess. Manag. 19, 571–573. https://doi.org/10.1002/ieam.4763.

Rivetti, C., Houghton, J., Rubio, M.B., Basili, D., Kukic, P., Muller, I., Hodges, G., Campos, B., 2025. Unlocking the future of environmental safety: a framework for integrating new approach methodologies in decision-making. NAM J. 1, 100028. https://doi.org/10.1016/j.namjnl.2025.100028.

SCCP. 2009. Opinion on triclosan - COLIPA No. P32. Report No. SCCP/1192/08, European Commission (EC) - Scientific Committee on Consumer Products (SCCP), https://ec.europa.eu/health/ph_risk/committees/04_sccp/docs/sccp_o_166.pdf.

SCCS. 2011. Opinion on triclosan-colipa n° P32: addendum to the SCCP opinion on triclosan (SCCP/1192/08) from January 2009. Report No. SCCS/1414/11, https://ec.europa.eu/health/scientific_committees/consumer_safety/docs/sccs_o_054.pdf.

SCCS. 2022. Scientific advice on the safety of triclocarban and triclosan as substances with potential endocrine disrupting properties in cosmetic products. Report No. SCCS/1643/22, https://health.ec.europa.eu/document/download/b43f36b5-6a19-4b76-88f5-6c1bf8fd8ade_en?filename=s.

Schaupp, C.M., Maloney, E.M., Mattingly, K.Z., Olker, J.H., Villeneuve, D.L., 2023. Comparison of *in silico, in vitro*, and *in vivo* toxicity benchmarks suggests a role for ToxCast data in ecological hazard assessment. Toxicol. Sci. 195, 145–154. https://doi.org/10.1093/toxsci/kfad072.

SCHEER, 2023. Final Opinion on Draft Environmental Quality Standards for Priority Substances Under the Water Framework Directive–Triclosan. Scientific Committee on Health, Environmental and Emerging Risks. https://health.ec.europa.eu/publications/scheer-scientific-opinion-draft-environmental-quality-standards-priority-substances-under-water-15_en.

Scholz, S., Renner, P., Belanger, S.E., Busquet, F., Davi, R., Demeneix, B.A., Denny, J.S., Leonard, M., McMaster, M.E., Villeneuve, D.L., Embry, M.R., 2013. Alternatives to *in vivo* tests to detect endocrine disrupting chemicals (EDCs) in fish and amphibians–screening for estrogen, androgen and thyroid hormone disruption. Crit. Rev. Toxicol. 43, 45–72. https://doi.org/10.3109/10408444.2012.737762.

Singer, H., Muller, S., Tixier, C., Pillonel, L., 2002. Triclosan: occurrence and fate of a widely used biocide in the aquatic environment: field measurements in wastewater treatment plants, surface waters, and lake sediments. Environ. Sci. Technol. 36, 4998–5004. https://doi.org/10.1021/es025750i.

Stasinakis, A.S., Kordoutis, C.I., Tsiouma, V.C., Gatidou, G., Thomaidis, N.S., 2010. Removal of selected endocrine disrupters in activated sludge systems: effect of

sludge retention time on their sorption and biodegradation. Bioresour. Technol. 101, 2090–2095. https://doi.org/10.1016/j.biortech.2009.10.086.
Suri, A., De Roy, C., Mishra, S., Autiero, M., Petry, T., 2025. P18-73 Application of SeqAPASS in the context of NAMs: supporting biomarker-based environmental hazard assessment. Toxicol. Lett. 411, S219. https://doi.org/10.1016/j.toxlet.2025.07.522.
Tanneberger, K., Knobel, M., Busser, F.J., Sinnige, T.L., Hermens, J.L., Schirmer, K., 2013. Predicting fish acute toxicity using a fish gill cell line-based toxicity assay. Environ. Sci. Technol. 47, 1110–1119. https://doi.org/10.1021/es303505z.
Tocher, D.R., 2003. Metabolism and functions of lipids and fatty acids in teleost fish. Rev. Fish. Sci. 11, 107–184. https://doi.org/10.1080/713610925.
US EPA. 2022. Methodology document for the ECOlogical Structure-Activity Relationship Model (ECOSAR) class program. Estimating toxicity of industrial chemicals to aquatic organisms using the ECOSAR (ECOlogical Structure-Activity Relationship) class program. Version 2.2. https://www.epa.gov/system/files/documents/2022-03/methodology-document-v.2.2.pdf.
US EPA, 2025. Estimation Programs Interface Suite™ for Microsoft® Windows, v 4.11. US Environmental Protection Agency. OnWashington, DC, USA. https://www.epa.gov/tsca-screening-tools/download-epi-suitetm-estimation-program-interface-v411 (accessed in May 2026).
US EPA. 2026a. CompTox chemicals dashboard v2.8.0: HTTr summary - triclosan (CAS number: 3380-34-5). https://comptox.epa.gov/dashboard/chemical/details/DTXSID5032498 (accessed in July 2025).
US EPA. 2026b. CompTox chemicals dashboard v2.8.0: ToxCast summary - triclosan (CAS number: 3380-34-5). https://comptox.epa.gov/dashboard/chemical/details/DTXSID5032498 (accessed in July 2025).
US EPA. 2026c. Toxicity forecasting (ToxCast): accessible bioactivity data for toxicology. https://www.epa.gov/comptox-tools/toxicity-forecasting-toxcast (accessed in July 2025).
Wetmore, B.A., Wambaugh, J.F., Ferguson, S.S., Sochaski, M.A., Rotroff, D.M., Freeman, K., Clewell 3rd, H.J., Dix, D.J., Andersen, M.E., Houck, K.A., Allen, B., Judson, R.S., Singh, R., Kavlock, R.J., Richard, A.M., Thomas, R.S., 2012. Integration of dosimetry, exposure, and high-throughput screening data in chemical toxicity assessment. Toxicol. Sci. 125, 157–174. https://doi.org/10.1093/toxsci/kfr254.
Wheeler, J.R., Grist, E.P., Leung, K.M., Morritt, D., Crane, M., 2002. Species sensitivity distributions: data and model choice. Mar. Pollut. Bull. 45, 192–202. https://doi.org/10.1016/S0025-326X(01)00327-7.
Wilburn, W.J., Gabure, S., Whalen, M.M., 2024. Interleukin 1beta and interleukin 6 production in human immune cells is stimulated by the antibacterial compound triclosan. Arch. Toxicol. 98, 883–895. https://doi.org/10.1007/s00204-023-03654-6.
Xin, X., Huang, G., An, C., Raina-Fulton, R., Weger, H., 2019. Insights into long-term toxicity of triclosan to freshwater green algae in lake erie. Environ. Sci. Technol. 53, 2189–2198. https://doi.org/10.1021/acs.est.9b00259.
Yang, L.H., Ying, G.G., Su, H.C., Stauber, J.L., Adams, M.S., Binet, M.T., 2008. Growth-inhibiting effects of 12 antibacterial agents and their mixtures on the freshwater microalga Pseudokirchneriella subcapitata. Environ. Toxicol. Chem. 27, 1201–1208. https://doi.org/10.1897/07-471.1.
Yoon, D.S., Choi, Y., Cha, D.S., Zhang, P., Choi, S.M., Alfhili, M.A., Polli, J.R., Pendergrass, D., Taki, F.A., Kapalavavi, B., Pan, X., Zhang, B., Blackwell, T.K., Lee, J. W., Lee, M.H., 2017. Triclosan disrupts SKN-1/Nrf2-mediated oxidative stress response in *C. elegans* and human mesenchymal stem cells. Sci. Rep. 7, 12592. https://doi.org/10.1038/s41598-017-12719-3.
Yoon, M., Clewell, H.J., 2016. Addressing early life sensitivity using physiologically based pharmacokinetic modeling and *in vitro* to *in vivo* extrapolation. Toxicol. Res. 32, 15–20. https://doi.org/10.5487/TR.2016.32.1.015.
Yu, G., He, Q.Y., 2016. ReactomePA: an R/Bioconductor package for reactome pathway analysis and visualization. Mol. BioSyst. 12, 477–479. https://doi.org/10.1039/c5mb00663e.
Zdrazil, B., 2025. Fifteen years of ChEMBL and its role in cheminformatics and drug discovery. J. Cheminform. 17, 32. https://doi.org/10.1186/s13321-025-00963-z.
Zhou, Z., Yang, J., Chan, K.M., 2017. Toxic effects of triclosan on a zebrafish (*Danio rerio*) liver cell line, ZFL. Aquat. Toxicol. 191, 175–188. https://doi.org/10.1016/j.aquatox.2017.08.009.